MARTIN MARIETTA ENERGY SYSTEMS LIBRARIES
3 4456 0352711 9

ORNL 910
Series A
Progress Report

AEC RESEARCH AND DEVELOPMENT REPORT

LABORATORY RECORDS
1954

METALLURGY DIVISION
QUARTERLY PROGRESS REPORT FOR PERIOD ENDING OCTOBER 31, 1950

OAK RIDGE NATIONAL LABORATORY
CENTRAL RESEARCH LIBRARY
CIRCULATION SECTION
4500N ROOM 175
LIBRARY LOAN COPY
DO NOT TRANSFER TO ANOTHER PERSON
If you wish someone else to see this report, send in name with report and the library will arrange a loan.
UCN-7969 (3 9-77)

DECLASSIFIED
CLASSIFICATION CHANGED TO:
BY AUTHORITY OF: AEC - 6-12-62
BY: N. Bowman 8.14.62

OAK RIDGE NATIONAL LABORATORY
OPERATED BY
CARBIDE AND CARBON CHEMICALS DIVISION
UNION CARBIDE AND CARBON CORPORATION
UCC
POST OFFICE BOX P
OAK RIDGE, TENNESSEE

[redacted]

ORNL-910

This document consists of 72 pages.
Copy 8 of 102. Series A.

Contract No. W-7405, eng 26

METALLURGY DIVISION

J. H. Frye, Jr., Director

QUARTERLY PROGRESS REPORT
for Period Ending October 31, 1950

Edited by

E. C. Miller and W. H. Bridges

DATE ISSUED FEB 8 1951

OAK RIDGE NATIONAL LABORATORY
operated by
CARBIDE AND CARBON CHEMICALS DIVISION
Union Carbide and Carbon Corporation
Post Office Box P
Oak Ridge, Tennessee

[redacted]

[redacted]

MARTIN MARIETTA ENERGY SYSTEMS LIBRARIES
3 4456 0352711 9

INTERNAL DISTRIBUTION

	G. T. Felbeck (C&CCD)
2-3	Chemistry Library
4	Physics Library
5	Biology Library
6	Health Physics Library
7	Metallurgy Library
8-9	Training School Library
10-13	Central Files
14	C. E. Center
15	C. E. Larson
16	W. B. Humes (K-25)
17	W. D. Lavender (Y-12)
18	A. M. Weinberg
19	J. A. Swartout
20	E. D. Shipley
21	E. J. Murphy
22	F. C. VonderLage
23	E. H. Taylor
24	F. L. Steahly
25	K. Z. Morgan
26	D. W. Cardwell
27	M. T. Kelley
28	W. H. Pennington
29	E. C. Miller
30	A. H. Snell
31	R. C. Briant
32	G. H. Clewett
33	W. H. Bridges
34	A. G. H. Andersen
35	L. R. Jetter
36	E. J. Boyle
37	W. D. Manly
38	C. D. Susano
39	W. W. Parkinson
40	R. J. Gray
41	B. S. Borie
42	D. S. Billington
43	C. D. Smith
44	D. E. Hamby
45	E. E. Stansbury
46	G. P. Smith
47	J. E. Cunningham
48	C. P. Keim
49-50	Central Files (O. P.)
51	Anton Brasunas

EXTERNAL DISTRIBUTION

52-59	Argonne National Laboratory
60-62	Atomic Energy Commission, Washington
63-66	Brookhaven National Laboratory
67-68	Knolls Atomic Power Laboratory
69-70	General Electric Company, Richland
71	Hanford Directed Operations
72-75	Los Alamos
76-77	New York Operations Office
78	Patent Branch, Washington
79-93	Technical Information Branch, ORE
94-97	University of California Radiation Laboratory
98	Massachusetts Institute of Technology (Kaufmann)
99	Battelle Memorial University
100-102	NEPA

[redacted]

TABLE OF CONTENTS

SUMMARY 7

I. MTR FUEL ELEMENTS 9

Introduction 9
Melting and Rolling 9
Fabrication 10
KAPL Disks 10

II. URANIUM BONDING STUDIES 12

Introduction 12
Silver-Mercury Bond Strength 12
Roll-cladding of Uranium with Copper 12

III. THORIUM ALLOY DEVELOPMENT 14

Introduction 14
Ternary Alloys of Thorium 14
Thorium Melting in Vacuum-arc Furnace 14
Impact Strength of Thorium 18
Yield Point in Thorium 22
Work-hardening of Thorium 24
Recrystallization of Thorium 24

IV. ALUMINUM-SILICON-URANIUM PHASE DIAGRAM WORK 28

V. AIRCRAFT NUCLEAR PROPULSION PROGRAM 29

Static Corrosion Testing 29

Stainless Steels in Lithium 29
Metallic Elements in Sodium 38
Materials in NaOH 38
Materials in Lead 39
Metal in Uranium-Aluminum Alloy 39

Dynamic Corrosion Testing 39

Forced Convection Loops 39
Thermal Convection Loops 41
Experimental Procedure 41
Chemical Analysis and Metallographic Examination 41
Auxiliary Equipment 41
Work in Progress 42
Procurement of Material and Loops 42

[redacted]

[redacted]

TABLE OF CONTENTS (Cont'd)

Compatibility Tests of Potential Fuel-element Materials 43

Description of Tests 43
Molybdenum—316 Stainless Steel 45
Molybdenum—309 Stainless Steel 45
Molybdenum-UO_2 45
Molybdenum-BeO 45
Columbium—316 Stainless Steel 45

Powder Metallurgy Laboratory 46

Formation of a Porous Structure by Selective Leaching 46

Welding Laboratory 47

Welding of Molybdenum 47
Welding of Columbium 47

Creep-rupture Laboratory 48

General 48
ANP Creep-rupture Testing 48
Creep of Uranium 48

VI. MECHANICAL PROPERTIES OF PURE METALS 50

VII. SERVICE WORK 65

Aluminum-Silicon Coated Slugs 65
Preparation of 5% Molybdenum—Uranium Alloy Sheet and Rod 66
Fabrication of Heater for Pile Fluxmeter 68
Uranium Melting 70
Welding Laboratory Service Work 70
Service Work of the MTR Group 71
Miscellaneous 71

METALLURGY DIVISION PERSONNEL 72

[redacted]

[redacted]

LIST OF TABLES

Table 1	Yields of Blister-free Plates	9
Table 2	Data for Binary Thorium Alloys	16
Table 3	Data for Ternary Thorium Alloys	17
Table 4	Impact Strength of Thorium	19
Table 5	Hardness of Cold-worked Thorium	24
Table 6	Corrosion of Stainless Steels in 1000°C Lithium	35
Table 7	Results of Contact of Potential Fuel-element Materials at 1100°C for 100 hr	44
Table 8	Comparison of Creep Curves and of Level Curves of the $(\sigma)_v$ Surface	63

[redacted]

[redacted]

LIST OF FIGURES

Fig. 1	Photomicrograph of 2% Be—98% Th Alloy as Cast	15
Fig. 2	Photomicrograph of 4% Al—96% Th Alloy as Cast	15
Fig. 3	Photomicrograph of 4% Si—96% Th Alloy as Cast	15
Fig. 4	Impact Energy for Pure Thorium, Standard V-notch Charpy Specimens	20
Fig. 5	Charpy Impact Tests on Thorium	21
Fig. 6	Thorium-Titanium Load-elongation Diagram	23
Fig. 7	Rate of Work Hardening of Thorium	25
Fig. 8	Isothermal Recrystallization Curves for Ames Thorium	27
Fig. 9-13	Effect of Time on Lithium Corrosion of Stainless Steel at 1000°C	30-34
Fig. 14	Corrosion Specimens in Molten U-Al Alloy	40
Fig. 15	Silhouette of Copper Specimen During Stress	51
Fig. 16	True Stress vs. Natural Strain Diagram, OFHC Copper, Room Temperature	52
Fig. 17	True Stress—Natural Strain Diagram, OFHC Copper, Specimen No. 2.292-40, Room Temperature, Strain Rate-0.005 in. per Hour or Less, Grain Size-0.030 mm	54
Fig. 18	True Stress—Natural Strain Diagram, OFHC Copper, Specimen No. 2.2911, Room Temperature, Beam Loading Type Creep Testing Machine, Loading Rate-¼ lb. per min. (1500 psi per hour)	55
Fig. 19	True Stress—Natural Strain Diagram, OFHC Copper, SR-4 Strain Gages, Strain Rate-0.005 in. per Hour or Less, Room Temperature, Grain Size-0.03 mm	56
Fig. 20	Deviations of $K_3\delta^m$ from Measured Stress, σ, OFHC Copper, Room Temperature	57
Fig. 21	OFHC Copper, 292 Series	59
Fig. 22	Level Curves of the $(\sigma)_v$ Surfaces, OFHC Copper, Room Temperature	61
Fig. 23	Rolled Plate of U-Mo Alloy	67
Fig. 24	Rate of Work Hardening of 5% Mo-U Alloy	69

[redacted]

[redacted]

SUMMARY

The production of modified MTR type fuel elements for the Bulk Shielding Facility has proceeded at a good pace. Minor changes in materials and methods have resulted in increased yields.

As yet, attempts to bond uranium to a cladding material have not resulted in bonds of sufficient strength, but work is continuing in an effort to develop bonds with high thermal conductivity and greater strength.

High thorium alloys with 2 to 4% Cb, Cr, Mn, Ti, Zr, Be, Al, and Si have been prepared. Those containing Be, Al, or Si are hard and brittle and are not cold-workable. The alloys with the other elements are cold-workable in the as-cast condition. The vacuum-arc furnace for melting thorium has been found to have an insufficient vacuum system to overcome outgassing. The addition of a booster pump is expected to correct this condition. The impact testing of commercially pure thorium using standard V-notch specimens has shown a transition from brittle to tough behavior in the range 120 to 200°C. The yield point previously reported in thorium has been examined in the light of the Cottrell theory, but as yet the results are inconclusive.

Work has started on the Al-Si-U diagram. Data being collected consist of UAl_4:UAl_3 ratios, lattice parameters, and microstructures. It has been found that for a 20% uranium alloy only 0.8% Si is necessary to completely suppress the formation of UAl_4.

The static corrosion testing of various materials in lithium, sodium, and lead at 1000°C continues. In general the ferritic iron-chromium alloys appear somewhat more resistant to corrosion by 1000°C lithium and lead than do the austenitic alloys. The results on stainless steels in 1000°C sodium are as yet inconclusive. The responsibility for the design and operation of the dynamic-corrosion-testing devices now rests with the ANP Engineering Group, the Metallurgy Division exercising metallurgical control. As runs are finished the rigs are to be turned over to the Metallurgy Division for examination.

Compatibility tests have been started as a guide in the selection of materials suitable for fuel-element fabrication. Combinations of molybdenum,

[redacted]

UO_2, BeO, columbium, and stainless steels 316 and 309 are in process of being tested. The method consists in enclosing materials in stainless-steel capsules, sealing, hot-swaging to 40% reduction, and heating for 100 hr at 1100°C.

The equipment for the welding laboratory is being received. The installation of the creep laboratory is continuing, and special machines and furnaces are being designed and built.

Part II of "A Study of Stress-Strain-Time Functions of Metals," containing the application of the ideas developed in Part I to results obtained experimentally on copper, is to be issued shortly.

Various service jobs have been done during the quarter.

I. MTR FUEL ELEMENTS

Introduction. During this period 28 modified MTR fuel elements were manufactured for use in the Bulk Shielding Reactor now under construction at ORNL. These differ from the standard MTR fuel unit in that there is no top positioning adapter and the bottom adapter has a round shape. Details are contained in a memorandum.[1]

Melting and Rolling. Yields of blister-free plates were high, averaging about 90%. The individual yields for each run are shown in Table 1.

TABLE 1

Yields of Blister-free Plates

RUN	TOTAL NO. OF PLATES	NO. OF BLISTERED PLATES	YIELD (%)
C37	58	3	95
C38	60	3	95
C39	60	3	95
C41	60	8	87
C42	60	2	97
C43	60	2	97
C44	60	3	95
C45	68	9	87
C46	68	9	87
C48	58	4	93
C49	54	7	87
Total	666	53	92 (avg.)

Several basic changes in technology were made during this period. Previously the feed material to the metallurgical operations was the oxide U_3O_8.

(1) Breazeale, W. M., *Fuel Elements for Bulk Shielding Facility*, CF-50-6-132 (June 23, 1950).

It was pointed out by J. M. Herndon (9212 Area, Y-12) that metal is almost as cheap to produce as U_3O_8, and, in addition, there is less danger of air contamination when metal is used. It was therefore decided to use the metal as raw material. Additional advantages of this change are (1) the melting time is reduced by a factor of 4; (2) crucible life is increased by a factor of about 10 because of lower melting temperature; (3) there is a reduction in the volume of wastes; and (4) no slag is necessary when metal is used.

Fabrication. Experiments to determine the feasibility of eliminating the drying or preheating step in fuel assembly fabrication have been discontinued because of the poor results obtained. It is possible to obtain good brazed joints without the drying or preheating part of the cycle. However, it was found that blisters are produced in the active plates if either of these steps is omitted. Five assemblies were brazed using the following cycle:

1. Dry 2 hr at 302°F.
2. Braze 50 min at 1110°F.

All assemblies showed blisters after brazing. Nine additional assemblies were then brazed with the addition of the preheating step, as follows:

1. Dry 2 hr at 302°F.
2. Preheat 50 min at 850°F.
3. Braze 38 min at 1110°F.

None of the above showed any blisters after brazing. Absolute humidity was uniformly high during this period, about 12×10^{-4} lb of H_2O per cubic foot.

These results indicate that it is necessary to dry the flux thoroughly at an elevated temperature to eliminate the possibility of blistering during brazing.

The blistered assemblies were disassembled after heating to brazing temperatures so that the plates could be remelted in later heats with a minimum of braze metal and aluminum.

KAPL Disks. At the request[2] of the AEC Reactor Development Division, 17,300 uranium-aluminum alloy disks were manufactured to be used in a critical

(2) Holland, A. H., Jr., *Fabrication of Enriched Alloy Washers for SIR-PPA*, CF-50-6-175 (June 30, 1950).

experiment at Knolls Atomic Power Laboratory. The specifications were:

16,000 disks 1.960 ± 0.004 in. in diameter

1,300 disks 1.922 ± 0.004 in. in diameter

Both sizes to contain a hole 0.194 ± 0.002 in. in diameter, the hole to be centered within 0.002 in.

Both sizes approximately 0.038 in. in thickness

U^{235} content 121 ± 4 mg/sq cm

~35% U-Al alloy

Permissible impurities same as for MTR

Plates of 2S aluminum or better, each to be stamped with batch number and individual identifying number

Details of fabrication are contained in a memorandum.[3] Briefly the operation was as follows: 35% U-Al alloy was melted, hot rolled (1200°F) to 0.042 in., and cold rolled to 0.038 in. Disks were then punched and weighed and the identifying number was stamped. The average yield of disks from any one ingot was about 55%. Scrap was recycled to the melting operation.

At the end of the run, a request was made for an extra allotment of disks amounting to 25% of the original order. When these are completed, a topical report will be issued covering the details of the fabrication.

It was noticed that about twenty disks blistered after standing at room temperature for one to two weeks. The blisters were elongated in the direction of rolling and were as much as five times the original disk in thickness. Inside these blisters was a deposit of a gray powder. As yet this has not been identified. X-ray diffraction patterns have been made and are being studied. Spectrographic analysis showed the main constituent to be aluminum with traces of copper, uranium, magnesium, manganese, silicon, iron, and calcium.

(3) Smith, C. D., *Request for Enriched Uranium for Preparation of U-Al Alloy Discs for KAPL*, CF-50-7-176 (Aug. 31, 1950).

II. URANIUM BONDING STUDIES

Introduction. Methods are being sought whereby the bond between a cladding material and uranium metal can be made to have greater strength and better heat-transfer characteristics.

Further tests on silver-mercury bonds show that they are quite weak. Shear strengths of the order of 4000 psi were obtained. Attempts to bond silver and uranium by roll-cladding have been successful. As-rolled samples have good bonds, as shown by chisel tests and bend-to-fracture tests. However, heating to elevated temperatures produces deterioration of the bond, probably because of compound formation.

Silver-Mercury Bond Strength. Experiments with bonding silver-plated uranium to silver-plated copper by heat and pressure, with mercury amalgamation of the adjoining surfaces, indicate that bond strengths of at least 4000 psi in shear may be expected. Specimens clamped in vises and heated in air at temperatures of 350, 450, and 550°C and for times of 2, 4, and 6 hr show an increase in bond strength with time at constant temperature and with increasing temperatures at a given time. Samples pressed in a hydraulic press at 5000 psi and 300°C for varying times are now being tested.

Roll-cladding of Uranium with Copper. Attempts were made to seal uranium in copper jackets for roll-cladding to avoid excessive oxidation of the uranium. The following three methods were used:

1. Silver-plated copper surfaces were bonded with mercury by hot-pressing (25,000 psi) for 2 hr at 350°C.
2. Same as (1), followed by torch-brazing with silver solder.
3. Same as (1), followed by furnace-brazing with silver solder.

It was found that the as-pressed silver-mercury bond was too weak to withstand the shearing stresses developed during rolling or the thermal stresses involved in torch-brazing. It was strong enough to maintain sealing during furnace-brazing.

Using this technique, three uranium-copper sandwiches were sealed and hot-rolled at 1000°F with reductions of 8:1, 10:1, and 16:1. Samples cut from

these plates were tested by bending back and forth until fracture occurred. In each case there was no separation of layers. As a further test, samples were clamped in a vise, and attempts were made to separate the layers with a chisel. A clean separation of the uranium and copper could not be obtained, indicating that the bond was at least as strong as the two joined metals.

Heating samples of these clad plates in air and in vacuum apparently causes deterioration of the bonding. Samples were heated at 150, 300, and 850°C in air and at 300, 600, and 850°C in vacuum. Metallographic X-ray diffraction and destructive tests are being run on these samples. Exposure in air at 300°C for 24 hr produces a noticeable weakening. Microexamination of samples heated in vacuum for ½ hr at 600°C showed evidence of compound formation at the silver-uranium interface. Heating samples to 850°C in air and in vacuum resulted in complete failure of the bond.

III. THORIUM ALLOY DEVELOPMENT

Introduction. Thorium alloy development work has been continued, with the major emphasis being placed upon the thorium-rich alloys containing Cb, Cr, Mn, Ti, and Zr. These alloys may be cold-worked in the as-cast condition. Samples were prepared for mechanical and physical testing, but the results are as yet incomplete. Alloys containing beryllium, aluminum, and silicon are hard and brittle and cannot be cold-worked, but it was thought that they might be hot-worked. Two thorium-beryllium billets were extruded at 900°C into 3/8-in. rod, but the excessive pressures required caused bending of the stem of the extrusion press and prevented further extrusion work at this time. It had been thought that after a preliminary hot-working to break up the cast structure, cold-working could be performed without cracking. However, the extruded rods were cracked without appreciable reduction when cold-rolled. Typical microstructures of alloys of thorium with beryllium, aluminum, and silicon are shown in Figs. 1, 2, and 3, respectively. Since these alloys apparently form intermetallic compounds which are inherently brittle, additional alloys were prepared with very small amounts of beryllium and silicon to reduce the amount of compound and still permit possible decarburization or deoxidation. The stoichiometric amounts of alloying elements necessary to completely use the oxygen and carbon in the Ames thorium is of the order of 0.5% by weight. Therefore alloys were prepared containing 0.25% and 0.50% beryllium and silicon for further study. The hardness and approximate melting points of the various alloys are shown in Table 2.

Ternary Alloys of Thorium. The ternary alloys Th-Si-Zr and Th-Ti-Zr were prepared, and the titanium alloy was rolled into 1/8-in. plate for corrosion-test studies. The alloys containing silicon could not be cold-rolled without excessive cracking. The results are given in Table 3.

Thorium Melting in Vacuum-arc Furnace. There have been two significant developments in the operation of the vacuum-arc furnace during the quarter. First, the power feeder was tried on powdered thorium. It did not work well because the gas content was too great for the capacity of the vacuum system, and, because the thorium was blown out of the crucible, there was very little powder actually added to the melt. A new feeder has been built which allows the material to be heated before being fed into the furnace.

Not Classified
Photo No. Y-2787

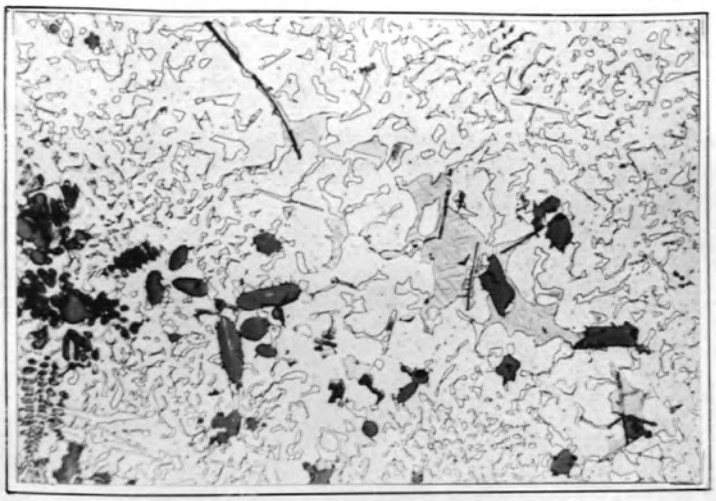

Y-2097 2% Be - 98% Th Alloy As Cast 500 X

Fig. 1

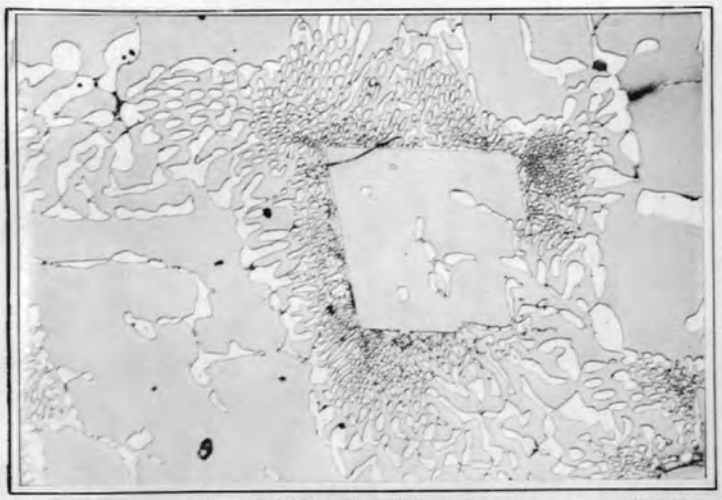

Y-2074 4% Al-96% Th Alloy As Cast 500 X

Fig. 2

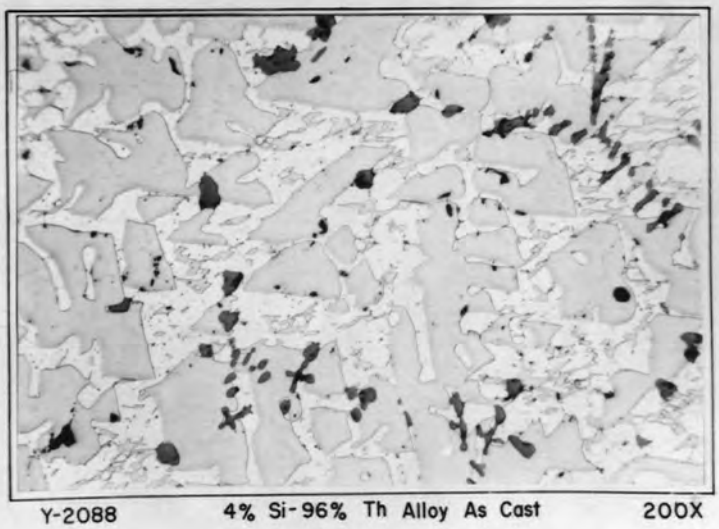

Y-2088 4% Si-96% Th Alloy As Cast 200X

Fig. 3

R. J. Gray - R. S. Crouse - E. P. Griggs

TABLE 2

Data for Binary Thorium Alloys

ALLOY NO.	COMPOSITION	APPROXIMATE MELTING POINT (°C)	HARDNESS		REMARKS
			DPH	ROCKWELL	
A-621	4% Ti	1405	64	RH 95	Cold-rolled, 75% reduction without cracking
A-624	6% Ti	1307	60	RH 93	Cold-rolled, 75% reduction without cracking
A-625	4% Cb	1500	76	RH 98	Cold-rolled, 75% reduction without cracking
A-627	6% Cb	1450	74	RB 24	Cold-rolled, 75% reduction without cracking
A-628	4% Cr	1310	131	RB 76	Cold-rolled, 75% reduction without cracking
A-629	6% Cr		108	RB 73	Cold-rolled, 75% reduction without cracking
A-630	0.25% In		135	RB 75	No rolling information
A-631	0.25% Be	1580	131	RB 68	No rolling information
A-632	0.25% Ce	1590		RB 62	No rolling information
A-633	0.25% Si	1560		RB 41	No rolling information
A-613	4% Zr	1565	69	RH 105	Cold-rolled, 75% reduction without cracking
A-614	6% Zr	1540	71	RH 103	Cold-rolled, 75% reduction without cracking

TABLE 3

Data for Ternary Thorium Alloys

ALLOY NO.	COMPOSITION	APPROXIMATE MELTING POINT (°C)	HARDNESS		REMARKS
			DPH	ROCKWELL	
A-543	1% Si, 1% Zr	1265	138	RB 80	Cracked after 10% reduction
A-551	1% Si, 2% Zr	1250	106	RB 57	Cracked after 10% reduction
A-556	1% Si, 4% Zr	1225	76	RB 41	Cracked after 10% reduction
A-561	2% Si, 1% Zr	1265	112	RB 71	Cracked after 10% reduction
A-566	4% Si, 1% Zr		116	RB 75	Cracked after 10% reduction
A-615	1% Ti, 1% Zr	1305	58	RH 91	Cold-rolled 75% reduction without cracking
A-616	1% Ti, 2% Zr	1300	64	RH 96	Cold-rolled 75% reduction without cracking
A-618	1% Ti, 4% Zr	1290	116	RH 110	Cracked
A-619	2% Ti, 1% Zr	1405	49	RH 91	Cold-rolled 75% reduction without cracking
A-620	4% Ti, 1% Zr	1330	70	RH 94	Cold-rolled 75% reduction without cracking

The second development was the use of a 12-channel oscillograph to record the following variables during the run: voltage, current, furnace pressure, fore-pressure, and electrode position. It was shown that the vacuum system is not entirely adequate for melting thorium and steel. It was found that the rate of gas evolution is almost constant during most of the run. The pressure in the furnace stays at about 1 to 2 μ Hg during the run but may become much higher when the arc reaches the top of the crucible and gives greater outgassing. A booster pump should be used so that greater capacity under heavier gas loads can be realized. Since the speed of the connection between the pump and furnace is only about 80 liters per second, the rate of outgassing is about 80 to 160 micron liters per second. This corresponds to about 60 to 125 cc per minute at standard conditions and represents about 1 to 2 cc of gas per cubic centimeter of melt.

Oscillography has also shown that the current and voltage are not functions of the arc gap, except that if the gap exceeds a certain length the arc collapses. This means that automatic control is very difficult. The method used for hand control is that of keeping the arc gap so small that metal dropping off shorts out the arc for a very short time, usually less than a tenth of a second. This shorting is most evident by the sound of the generator rather than by the arc intensity. The method gives good results but it is not necessarily the best that could be developed. A method of automatic control would have to work on the same principle unless some other method could be found.

The design of a new vacuum-arc furnace is dependent upon what can be found out about the operation of the new feeder and the water-cooled electrode; these have not yet been tried.

Impact Strength of Thorium. Previous work on impact strength of thorium has resulted in erratic results, perhaps due to a combination of imperfect samples and improper testing techniques. A single piece of rolled thorium was machined into standard V-notch Charpy type specimens for further testing. The samples were fully annealed and brought to the proper testing temperature, using liquid nitrogen for -196°C, dry ice and acetone for -80°C, ice water for 0°C, room temperature for 20°C, boiling water for 100°C, and an oil bath for higher temperatures. The specimens were handled with tongs which were at the

same temperature as the specimen and were quickly placed in the machine, where they were immediately broken. The testing temperature was therefore essentially the same as the bath temperatures.

The actual testing temperatures and the impact strength of thorium at these temperatures is given in Table 4. The impact energy in foot-pounds is plotted as a function of temperature in Fig. 4. The scatter found in earlier data has been eliminated, and a relatively smooth curve is obtained, showing that commercially pure thorium tested by notched-bar impact tests exhibits a transition from brittle to tough behavior, i.e., impact strength increases with increasing temperature over a moderately narrow range of temperature. The types of fracture found in the temperature range studied are shown in Fig. 5.

TABLE 4

Impact Strength of Thorium

TEMPERATURE (°C)	FOOT-POUNDS TO BREAK SPECIMEN
-195	11.5; 13.5
-80	13.5; 15.0
-60	15.0
-40	18.0
-20	19.0
0	20.0
20	21.0; 22.0
60	22.0; 23.0
100	31.0
120	44.0
130	50.0
140	59.0; 61.0
150	66.0
160	69.0; 71.0
170	78.0
180	88.0
190	99.0
200	108.0; 107.0
220	114.0; 114.0
240	Specimen not broken at limit of machine (120 ft-lb)

[redacted]

DWG. 10312

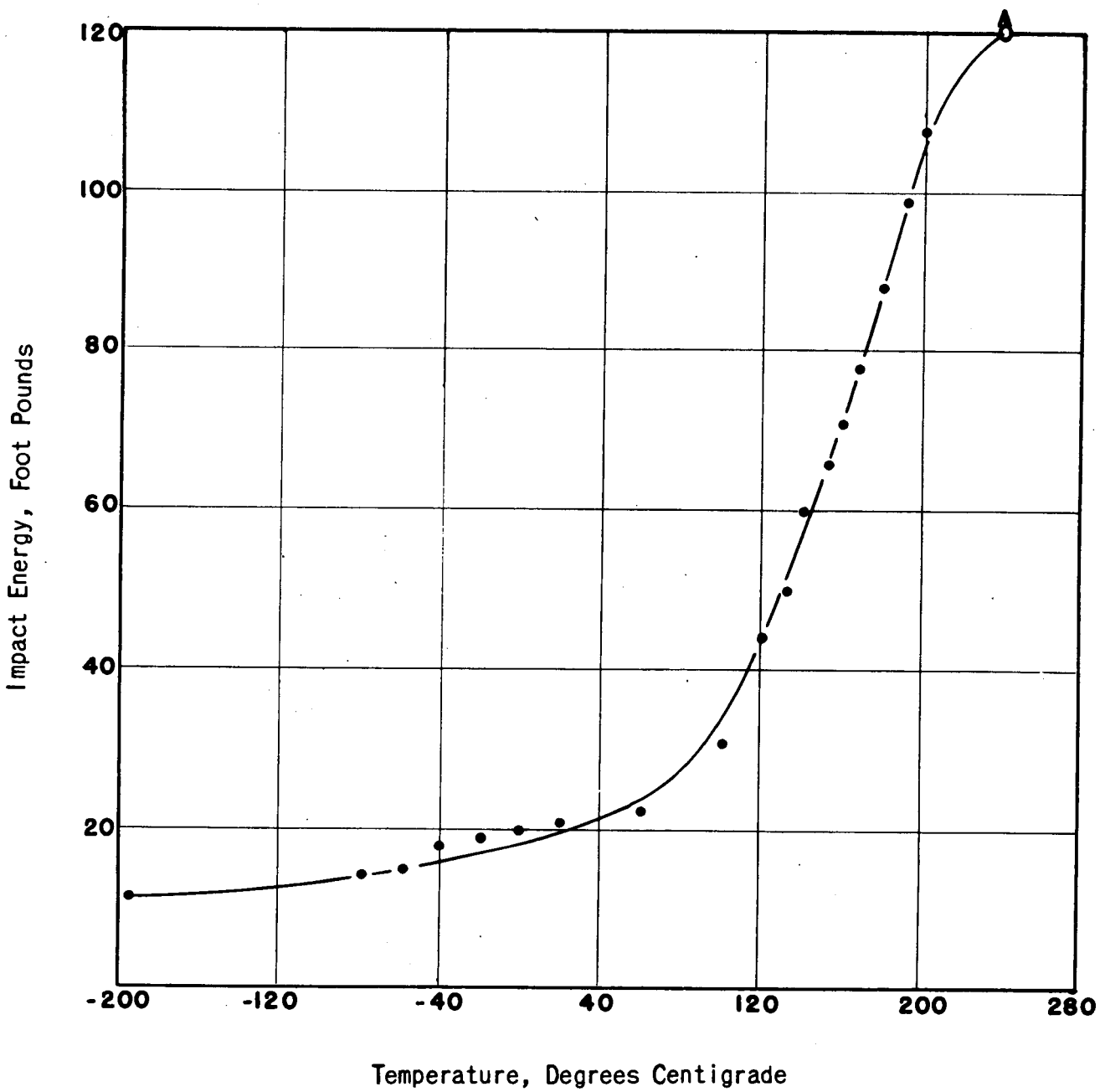

FIGURE 4

IMPACT ENERGY FOR PURE THORIUM
STANDARD V-NOTCH CHARPY SPECIMENS

NOT CLASSIFIED
PHOTO NO. Y-2433

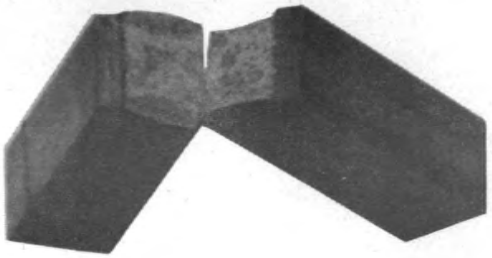

− 195°C
12 Foot Pounds

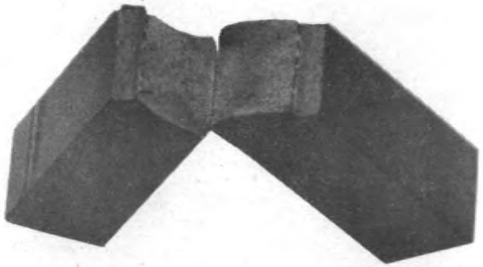

− 80°C
14 Foot Pounds

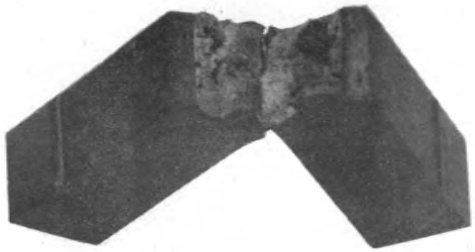

− 0°C
21 Foot Pounds

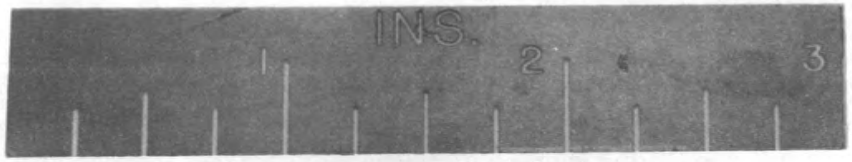

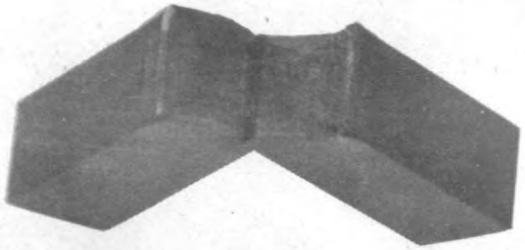

60°C
23 Foot Pounds

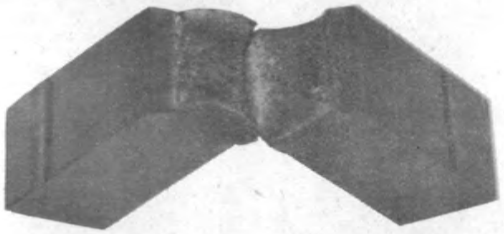

120°C
44 Foot Pounds

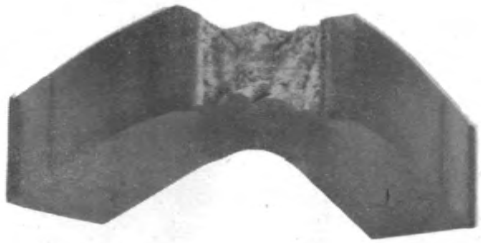

240°C

CHARPY IMPACT TESTS ON THORIUM
Fig. 5

Yield Point in Thorium. An apparent yield point in thorium has been reported (ORNL 827), and this phenomenon has been further studied by tensile tests on thorium melted in an atmosphere of nitrogen. It was hoped that a high nitrogen content might accentuate the yield point since it has been shown that nitrogen is a contributing factor in the appearance of a yield point in low-carbon steel and in single crystals of cadmium and zinc.[1] A recent theory (Cottrell, 1948) suggests that the yield point is caused by the segregation of solute atoms (nitrogen) to dislocations. The attraction of dislocations to the segregated atoms provides a bond which has to be broken by a larger force than is necessary to maintain freed dislocations in motion; the material thus gives way suddenly and softens at the start of plastic flow, producing a sharp yield point. The theory also explains the observed removal of the yield point by plastic overstrain and its return on strain aging. A freshly strained specimen contains freed dislocations and does not show a yield point, but on aging these dislocations become anchored by migration of solute atoms to them, and the yield point returns.

The Ames thorium used for these tests contained approximately 0.02% nitrogen, while the thorium melted in an atmosphere of nitrogen contained 0.3% nitrogen. Attempts to fabricate tensile specimens by cold-rolling failed because of the embrittlement associated with the high nitrogen content. A cast ingot was therefore machined into a standard round specimen and tested. No yield point was observed since there was no detectable plastic flow and the sample failed with a brittle break. Thorium-titanium and thorium-zirconium alloys were prepared to determine the effect of alloying on the yield point. Insufficient samples were available to perform careful tests with duplicate specimens, but, on the basis of the limited number of tests, it appears that titanium might possibly remove the yield point of thorium. Testing will be continued as additional samples become available. Presumably the titanium could tie up the nitrogen or carbon and prevent their migration to the dislocations. The load elongation diagram of thorium-titanium is shown in Fig. 6. Thorium which had been cold-worked slightly to remove the yield point was aged at room temperature in an attempt to cause the yield point to return. The specimen which was aged for the maximum time of 84 days did not show a yield point, so another specimen which has been aged at room temperature for 84 days was heated in boiling water for 1 hr and tested. Since the yield point was not found in this sample, more test bars are being prepared to age at elevated temperatures but below the recrystallization temperature.

(1) Wain, H. L., and Cottrell, A. H., "Yield Points in Zinc Crystals," *Proc. Phys. Soc* (B) 63, 339 (1950).

[redacted]
DWG. 10309

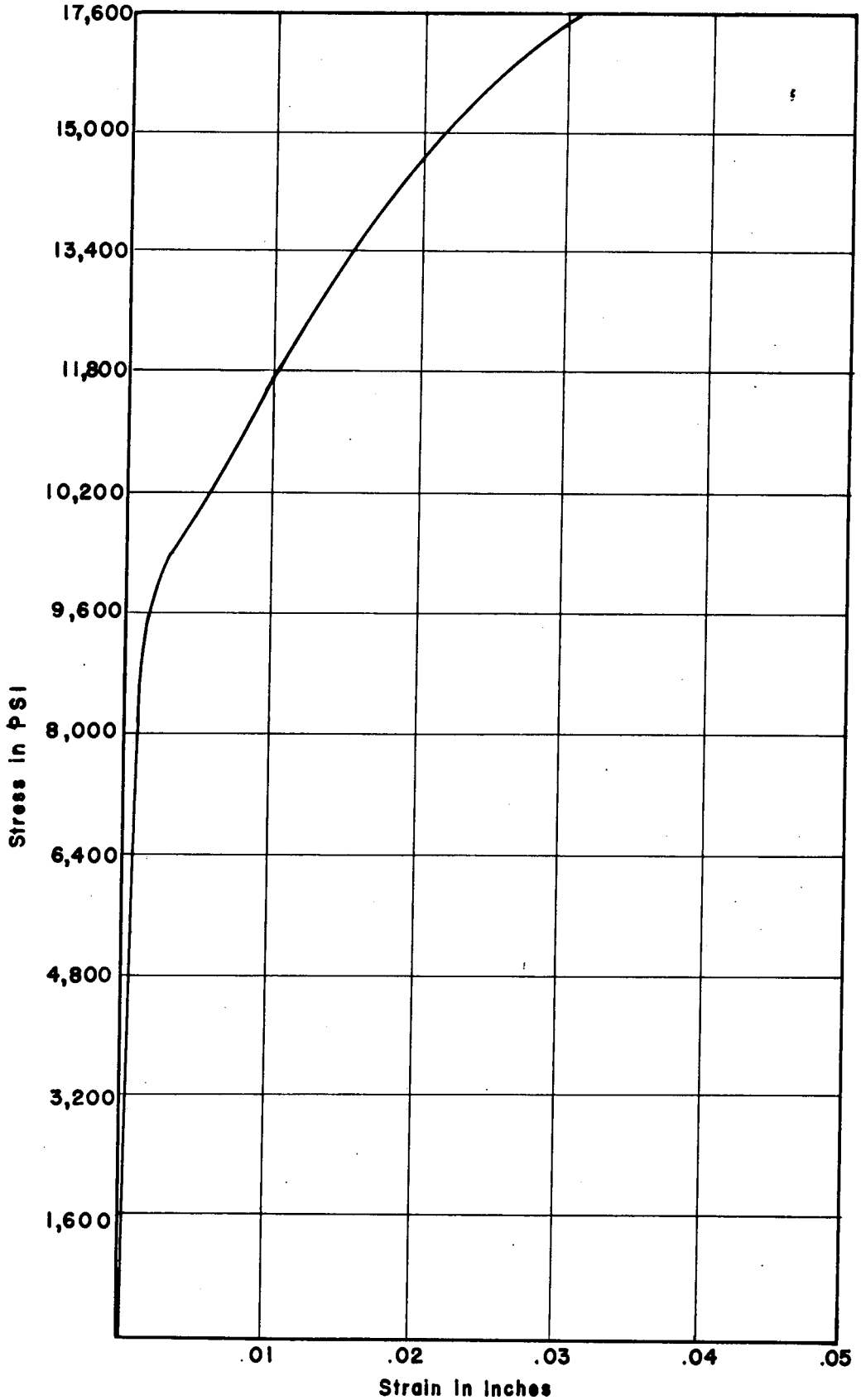

FIGURE 6

THORIUM-TITANIUM LOAD ELONGATION DIAGRAM

Work-hardening of Thorium. It has been noted that thorium does not work-harden to any great extent during cold-rolling since it may be reduced as much as 99% without an intermediate annealing and without extreme change in hardness. Preliminary tests on the rate of work-hardening of thorium showed that most of the hardening occurred very early in the rolling operation. Therefore, a piece of thorium was cold-rolled to 99.9% reduction with pieces being cut from the original thorium after each 5% reduction. Owing to the initial high rate of work-hardening, smaller increments of cold-working were used, up to 10% cold-working. The hardness data and degree of cold-working are shown in Table 5. Beyond 10% cold-working the rate of work-hardening is very small, as shown graphically in Fig. 7. The total change in hardness, even with large amounts of cold-working, is comparatively small (DPH 85 to 135). Different lots of thorium also give different results in that the maximum attainable hardness is sometimes less than that shown in Fig. 7. This presumably is due to differences in purity of the thorium.

TABLE 5

Hardness of Cold-worked Thorium

DEGREE OF COLD-WORKING (% Reduction)	DPH	DEGREE OF COLD-WORKING (% Reduction)	DPH
0	87.0	45	120.0
2	108.0	50	120.5
4	112.0	55	121.0
6	113.2	60	121.5
8	114.0	65	122.3
10	115.0	70	123.5
15	116.0	75	124.2
20	117.0	80	125.3
25	118.0	85	127.1
30	118.5	90	129.0
35	119.0	95	131.0
40	119.5	99.9	135.0

Recrystallization of Thorium. The study of the recrystallization of thorium has been continued by determination of recrystallization curves obtained by measuring the changes of hardness found after heating cold-worked

[redacted]
DWG. 10311

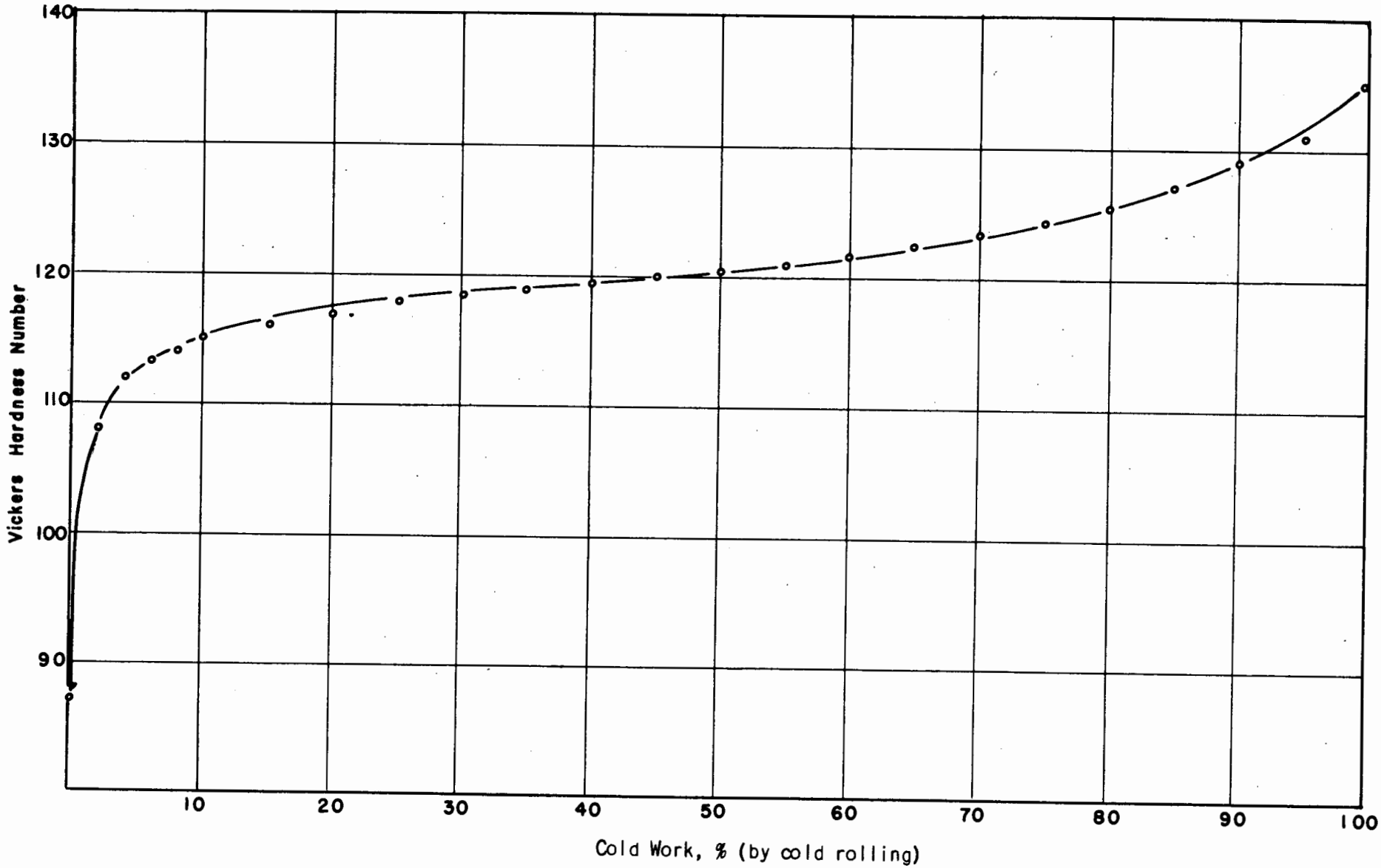

FIG. 7

RATE OF WORK HARDENING OF THORIUM

thorium at constant temperatures for varying lengths of time. There are considerable differences in the hardness of different lots of thorium after the same amount of deformation; thus the curves do not always start from the same value of hardness. This anomaly will be more thoroughly investigated in the future. Typical recrystallization curves are shown in Fig. 8, which shows the time dependence of the recrystallization at different amounts of cold-working. This study will be continued to determine the isothermal recrystallization curves of thorium at various temperatures and at different degrees of cold-working.

[redacted]
DWG. 10310

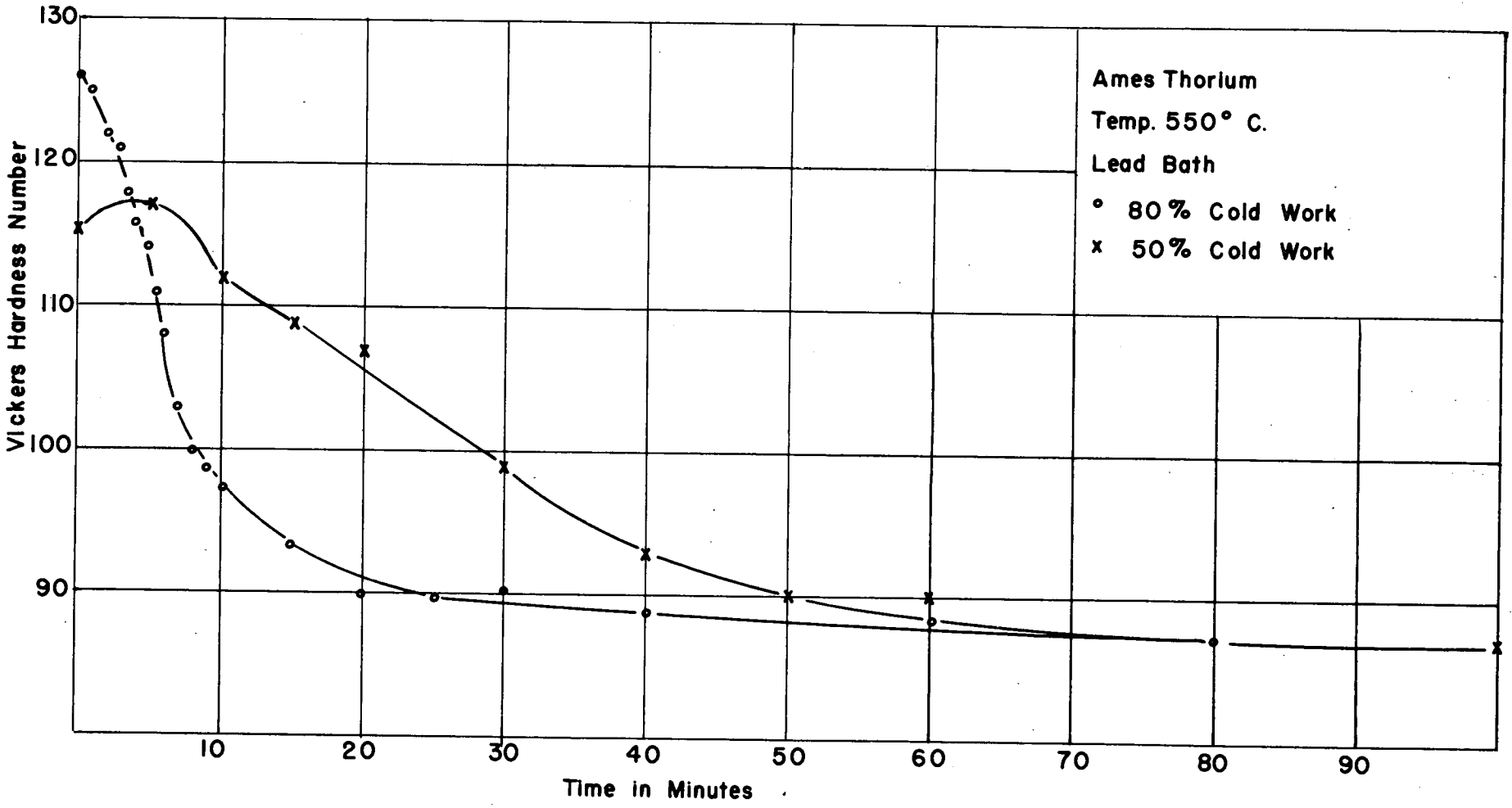

FIG. 8

ISOTHERMAL RECRYSTALLIZATION CURVES
FOR AMES THORIUM

IV. ALUMINUM-SILICON-URANIUM PHASE DIAGRAM WORK

During the past quarter alloys have been made up to study the aluminum-rich part of the ternary Al-Si-U phase diagram. This is important since it is known that a small amount of silicon will alter the uranium-bearing phase in alloys of uranium and aluminum. It suppresses the formation of UAl_4 and promotes the formation of UAl_3, which can exhibit a shifted lattice parameter owing to the substitution of the silicon for the aluminum in this phase. This has a number of important effects, such as increasing the density of the uranium-bearing phase and possibly shifting the eutectic composition toward the aluminum side. All this may be important in radiation damage since it is believed that particle size is important. It also permits the use of alloys which have somewhat different physical properties.

No attempts have been made to determine the diagram above the triple eutectic point, or uranium percentage higher than that in USi_3. The data being collected consist of determinations of the relative amount of UAl_4 to UAl_3, lattice parameters, and microstructures for 20% uranium alloys, containing up to 30% silicon.

The results are far from being complete but the following facts are known: The presence of the uranium does not lower the aluminum-silicon eutectic temperature by more than one degree since there was no detected change. Using 20% uranium, only about 0.8% silicon is required for complete suppression of the UAl_4. The boundaries of the three-phase region are approximately $U(Al_{0.96}\ Si_{0.04})_3$, Si, and $Al_{0.99}\ Si_{0.01}$. The boundary points of aluminum and silicon are believed to be the same as those for the aluminum-silicon binary system since solution of uranium has not been detected in either. It seems that the point $U(Al_{0.96}\ Si_{0.04})_3$ is a function of temperature and that this is only an average value.

V. AIRCRAFT NUCLEAR PROPULSION PROGRAM

STATIC CORROSION TESTING

Stainless Steels in Lithium. In an effort to study the time dependence of the corrosion of stainless steels, several commercial alloys were tested in 1000°C lithium for periods of 4, 40, and 400 hr. The alloys tested included the chromium steels 405, 430, and 446 as well as the austenitic grades 304, 310, 316, and 347.

Tests were conducted in the usual manner of sealing the test specimen plus a controlled amount of lithium in an evacuated Armco capsule, heating to the desired temperature, and holding the test capsule at this temperature for the specified time. The source of lithium was the low-sodium grade supplied by Metalloy Corporation of Minneapolis, Minn. The test specimen-to-lithium volume ratio varied slightly between 0.5 and 0.7. All tests were run in triplicate.

The 400-hr test results are tabulated, together with the 4- and 40-hr results reported last quarter, in Table 6. Weight-change data are reported as an average of the three specimens tested. Penetration measurements were made metallographically, and the bath metal, after the test, was analyzed spectrographically.

Comparison photomicrographs showing the effect of time on the corrosion are presented in Figs. 9 through 12. For convenience, the nature and depth of attack of each of the seven stainless-steel alloys tested are shown on the bar graph in Fig. 13.

Metallographic and X-ray examination indicated the following concerning the corrosion of commercial stainless steels by high-temperature lithium:

1. Attack is largely intergranular in nature. There is some surface removal.

2. In the 18-8 type stainless-steel alloy, areas adjacent to attacked grain boundaries and similar exposed surfaces undergo a phase transformation from austenitic to ferritic. This is presumably due to solution or diffusion of an austenite former, such as carbon or nickel, into lithium.

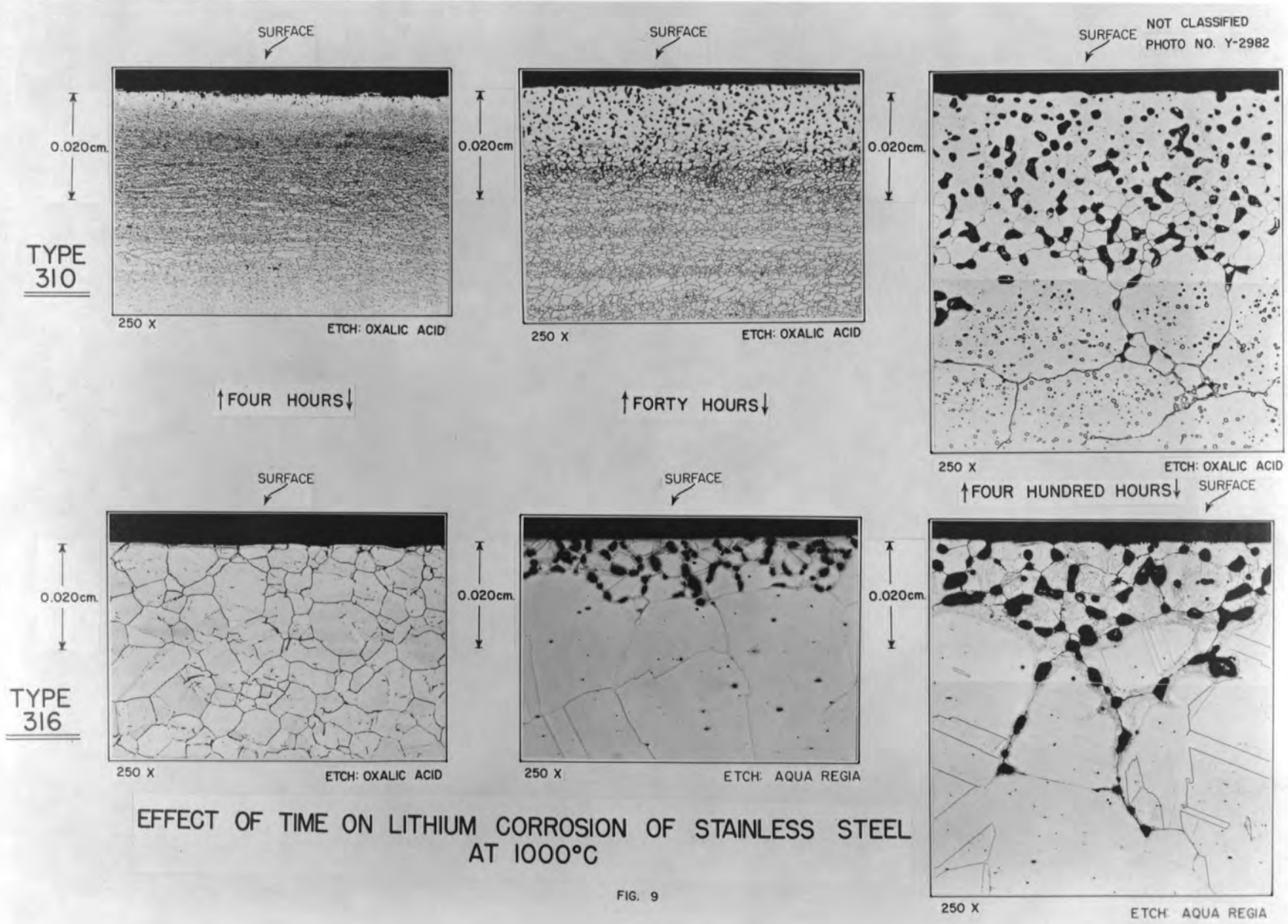

EFFECT OF TIME ON LITHIUM CORROSION OF STAINLESS STEEL AT 1000°C

FIG. 9

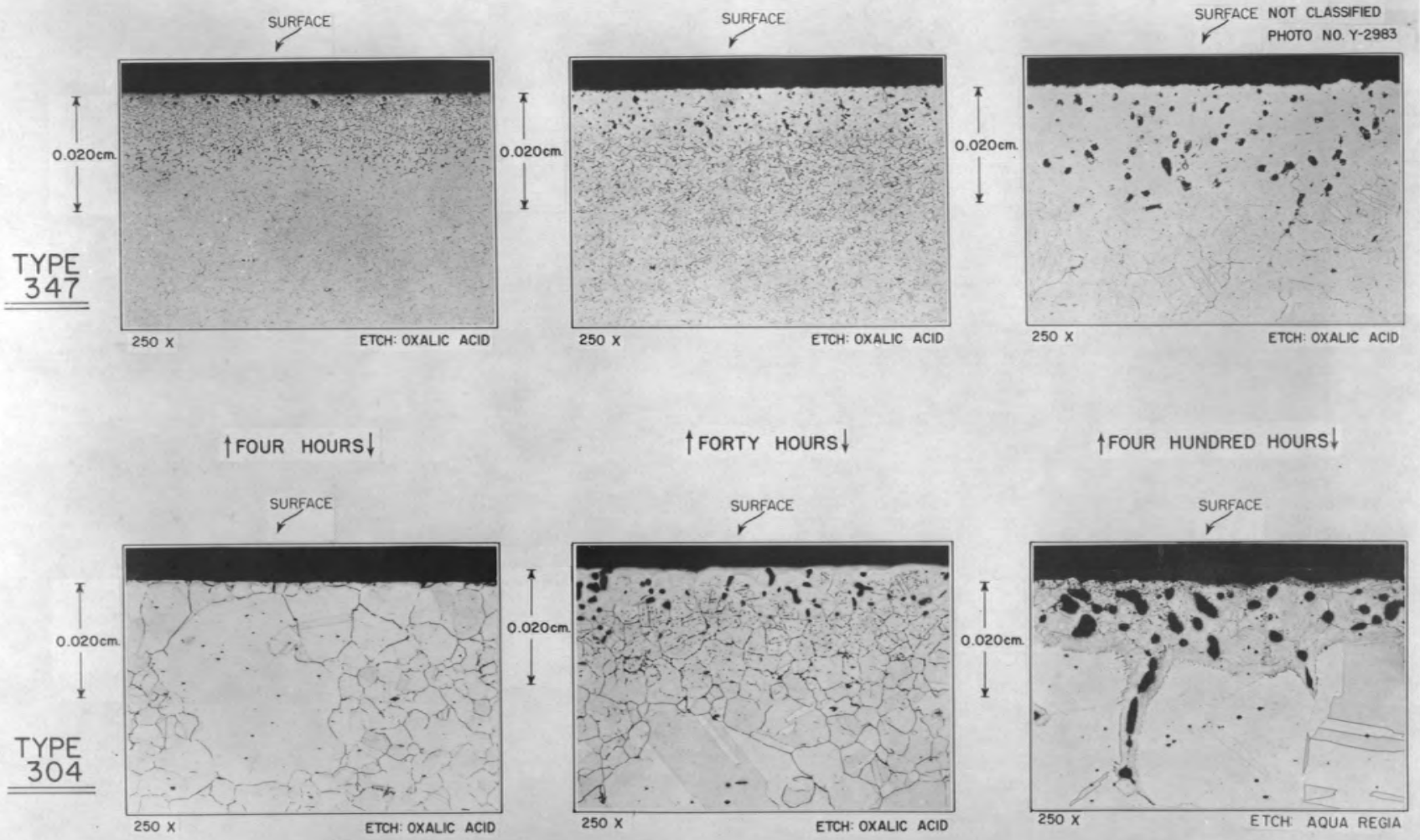

EFFECT OF TIME ON LITHIUM CORROSION OF STAINLESS STEEL AT 1000°C

FIG. 10

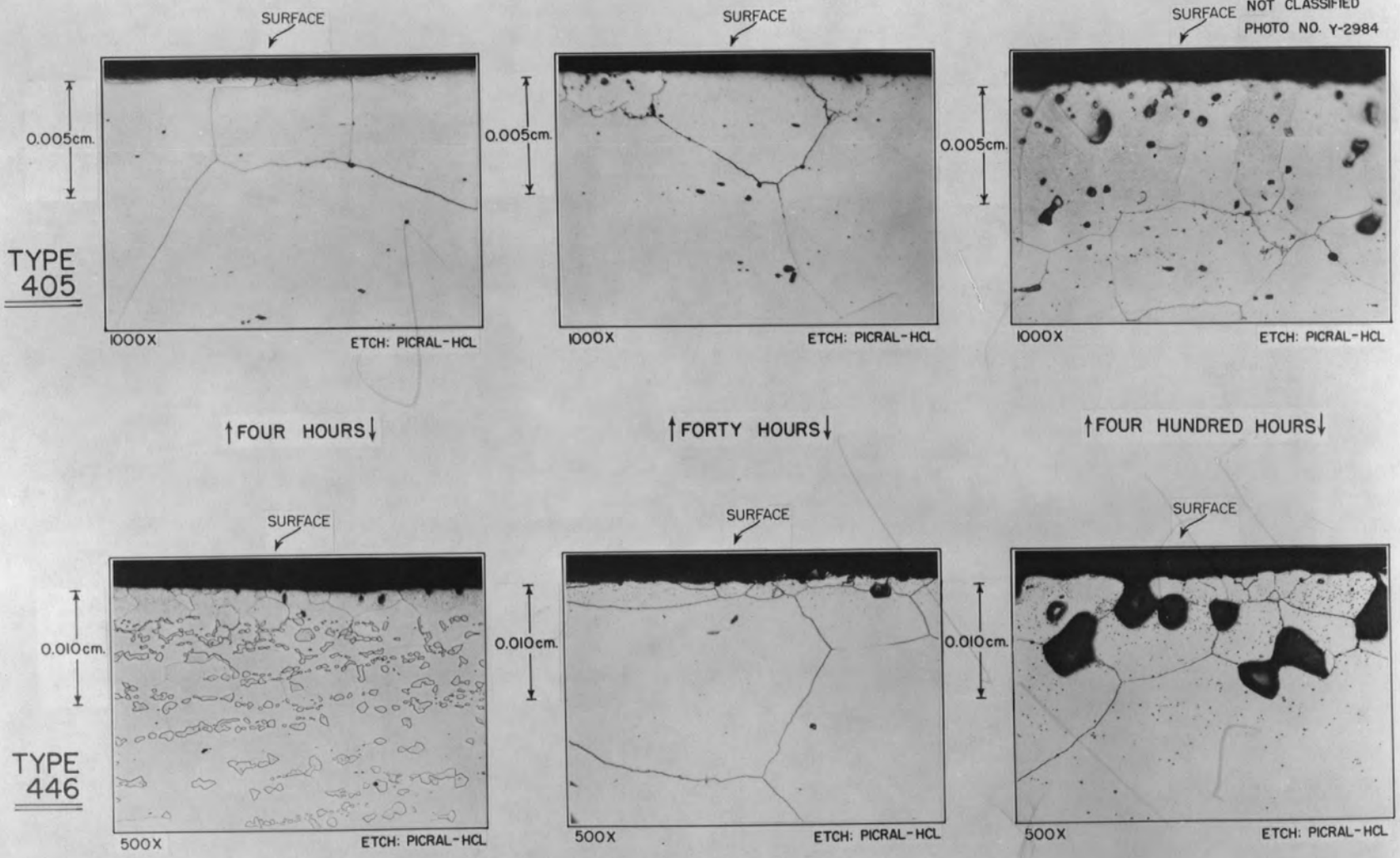

EFFECT OF TIME ON LITHIUM CORROSION OF STAINLESS STEEL AT 1000°C

FIG. 11

NOT CLASSIFIED
PHOTO NO. Y-2985

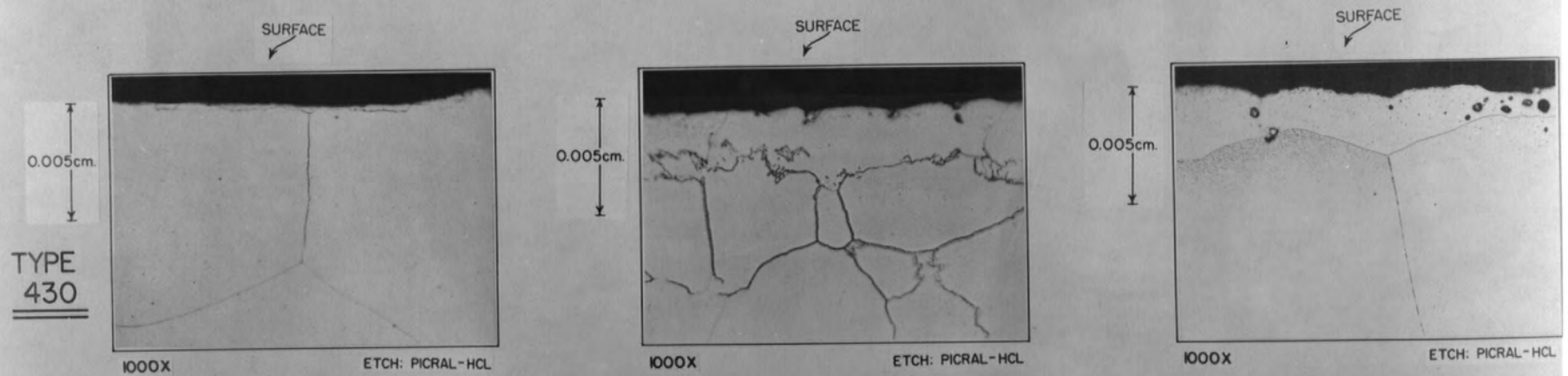

FOUR HOURS

FORTY HOURS

FOUR HUNDRED HOURS

EFFECT OF TIME ON LITHIUM CORROSION OF STAINLESS STEEL AT 1000°C

FIG. 12

DWG. 9925
NOT CLASSIFIED

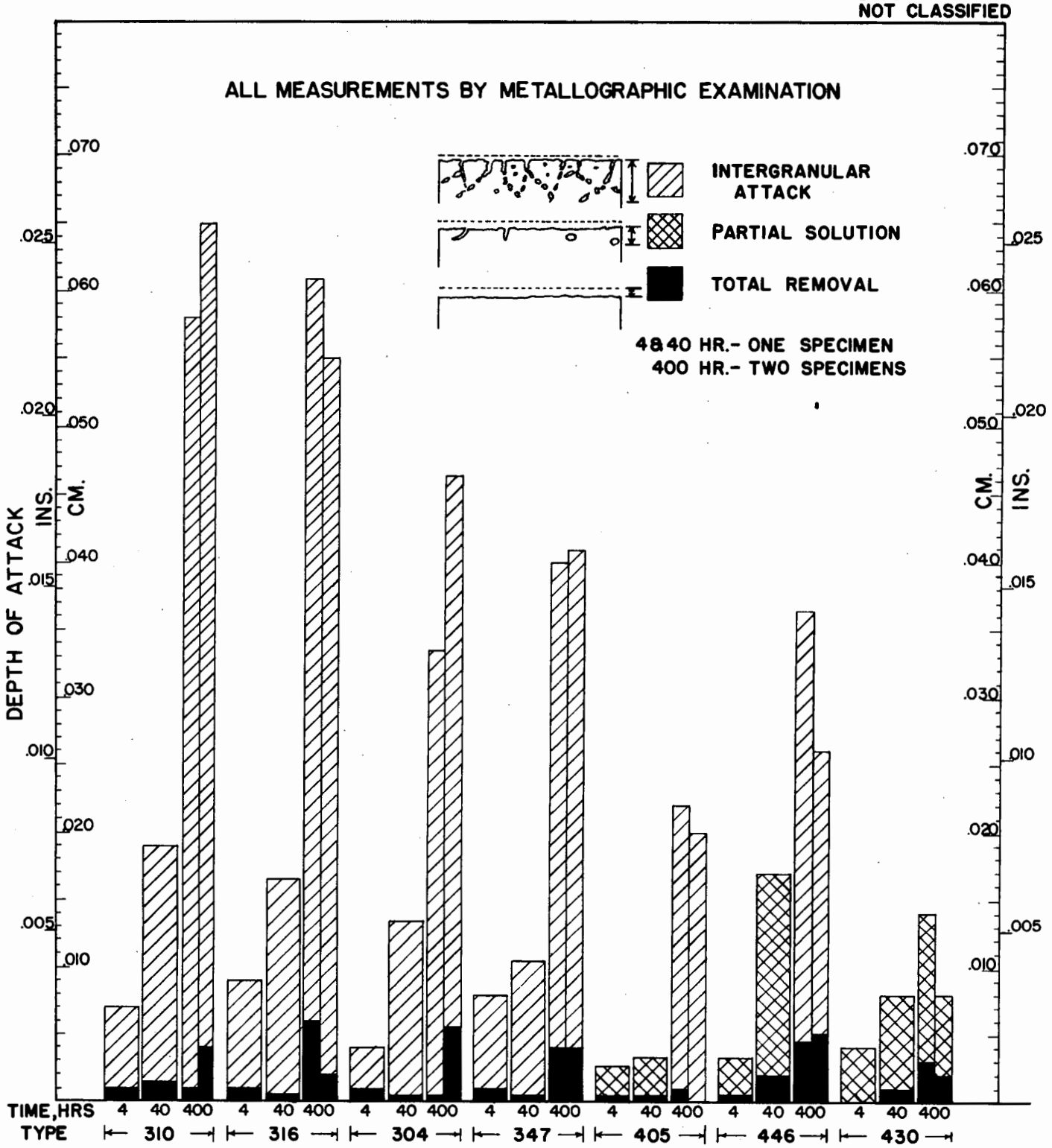

EFFECT OF TIME ON LITHIUM CORROSION OF STAINLESS STEEL AT 1000°C

R.J.G.

FIG. 13

TABLE 6

Corrosion of Stainless Steels in 1000°C Lithium

(Specimen Size 1 by 3/4 by 1/4 in.)

STAINLESS STEEL NO.	NO. OF SAMPLES TESTED	TEST DURATION (hr)	AVG. WT. CHANGE (mg/cm^2)	PENETRATION (mils)	BATH ANALYSIS AFTER TEST* (Range in ppm)	REMARKS
304	3	4	-1.39	2	Fe-20-57 Ni-ND-110 Cr-ND-57 Mn-ND	Microphotograph shows intercrystalline attack and evidence of phase transformation at grain boundaries; X-ray examination showed a ferritic surface; moderate resistance for short exposures, poor resistance for long exposures
	3	40	-5.62	6	Fe-20-90 Ni-90-250 Cr-ND	
	3	400	-16.06	15	Fe-570 Cr-44 Ni-ND Mn-9.3	
304LC	3	400	-65.56	No data	No data	X-ray diffraction examination showed both α and γ iron; specimens had an etched appearance and apparently the attack was uniform
310	3	4	-1.56	2.5	Fe-20-70 Ni-140-250 Cr-ND	Fair resistance for short exposures, poor resistance for long exposures; microscopic examination showed excessive solution of material in grain boundaries; X-ray examination showed both ferrite and austenite on the surface
	3	40	-30.75	7	Fe-25-54 Ni-310-450 Cr-ND	
	3	400	-64.76	25	Fe-180 Ni-110 Cr-41 Mn-77	

TABLE 6 (Cont'd)

STAINLESS STEEL NO.	NO. OF SAMPLES TESTED	TEST DURATION (hr)	AVG. WT. CHANGE (mg/cm^2)	PENETRATION (mils)	BATH ANALYSIS AFTER TEST* (Range in ppm)	REMARKS
316	3	4	-1.56	4	Fe-25-45 Ni-ND-140 Cr-ND-53 Mo-ND	Moderate resistance for short exposures, very poor for long exposures; microscopic examination showed excessive solution of material in grain boundaries in 40- and 400-hr exposures; evidence of phase transformation near surface at attacked grain boundaries; X-ray examination showed a ferritic structure
	3	40	-6.70	7	Fe-23-71 Ni-91-270 Cr-ND	
	3	400	-25.27	22	Fe-91 Ni-ND Cr-26 Mo-ND	
347	3	4	-1.97	3	Fe-25-70 Ni-ND-730 Cr-ND-12 Nb-ND	Moderate resistance to attack; microscopic examination showed some solution of material in grain boundaries near the surface; possible phase transformation near attacked grain boundaries; X-ray examination showed a ferritic structure
	3	40	-10.49	4	Fe-25-60 Ni-170-200 Cr-, Nb- } ND	
	3	400	-27.24	15	Fe-420 Ni-25 Cr-22 Nb-270 Mn-7	
405	3	4	-1.09	1	Fe-25-37 Al-, Cr- } ND	Good resistance; microscopic examination showed practically no intercrystalline attack; some partial solution at surface; indications of attack of some constituent within the grains near the surface; X-ray examination showed ferrite
	3	40	-3.44	1	Fe-73-150 Cr-ND	
	3	400	-8.36	7	Not reported	

TABLE 6 (Cont'd)

STAINLESS STEEL NO.	NO. OF SAMPLES TESTED	TEST DURATION (hr)	AVG. WT. CHANGE (mg/cm^2)	PENTRATION (mils)	BATH ANALYSIS AFTER TEST* (Range in ppm)	REMARKS
430	3	4	-1.26	2	Fe-19-32 CR-ND	Good corrosion resistance; microscopic examination showed practically no evidence of intercrystalline attack; partial solution on long exposure; X-ray examination showed ferrite
	3	40	-4.13	3	Fe-23-40 Cr-ND	
	3	400	-9.89	4	Not reported	
446	3	4	-3.24	1	Fe-14-53 Cr-ND-37 Mn-3.7-19 Al-150	Moderate resistance during short exposures; microscopic examination showed heavy solution at grain boundaries; some decarburization and grain growth at exposed surface; X-ray examination showed ferrite
	3	40	-9.79	7	Fe-34-150 Cr-ND	
	3	400	-9.89	13	Not reported	

* ND = not detected.

3. Decarburization of the structure in immediate contact with molten lithium was observed.

4. Both the ferritic and austenitic grades showed grain growth with increasing time. The grain coarsening was largely confined to the parent metal with little or no effect on the zone that was directly attacked.

5. In general, the ferritic iron—chromium alloys appear to be more resistant to lithium at 1000°C than do the austenitic grades.

Results of the corrosion tests that were completed indicate that ordinary commercial stainless-steel alloys will not be suitable for containing molten lithium at a service temperature of 1000°C. Tests are in progress to determine the behavior of these alloys at temperatures of 700 and 850°C. Extra-low-carbon grades in all obtainable stainless-steel alloys are also being tested.

Metallic Elements in Sodium. Tests were initiated on several elements and alloys to determine their corrosion resistance to sodium at high temperatures. The sodium used for these tests was of commercial purity (99.95%) obtained from Merck and Company. In the first tests the specimens were enclosed in Armco iron capsules. Examination of the capsules showed that the sodium had leaked through the capsule bottoms sometime during the test period, and it was concluded that Armco would not contain sodium.

Next, tests were made using nickel capsules, and it was found that this material, if properly welded, would contain sodium. Since this time the sodium tests have been in evacuated nickel or stainless-steel capsules. Preliminary inspection, on a basis of weight-change data only, indicates that nickel shows good resistance, and that cobalt, molybdenum, tantalum, alloy N-155, inconel, and inconel X show fair resistance to sodium for 400 hr at 1000°C. The stainless steels are also being studied extensively, in the form of both flat stock and tubing, in high-temperature sodium. When metallographic examination of the specimen is completed, more detailed information will be reported.

Materials in NaOH. During the quarter work on this coolant has been confined to searching for reliable methods to produce a low-carbonate water-free grade of sodium hydroxide. Further evaluation of the preliminary tests (4 hr at 1000°C) showed that iron, zirconium, columbium, and tantalum completely dissolved in Baker's chemical reagent grade, 98.9% assay NaOH. The

austentic stainless steels (grades 304, 310, 316, and 347), as well as the high-temperature alloys L-605 and V-36, were characterized by an exfoliation type of attack. Of the metallic materials tested, only the nickel capsules showed promise of resisting NaOH at 1000°C.

In the coordinated ORNL-NEPA materials program, the problem of finding suitable materials for containing molten NaOH will be largely the responsibility of the NEPA Chemistry Section.

Materials in Lead. Interest in the use of molten lead as a heat-transfer fluid in the proposed ARE has increased recently.

Preliminary tests completed last quarter on some of the metallic elements indicated moderately good resistance of tungsten, zirconium, iron, and tantalum; fair resistance of molybdenum and beryllium; and poor resistance of titanium and nickel exposed to lead at 1000°C for 40 hr. Additional tests are in progress to determine the resistance of stainless-steel alloys in contact with lead at 1000°C. Particular emphasis is being given to the straight chromium ferritic stainless-steel alloys and extra-low-carbon grades of these.

Metal in Uranium-Aluminum Alloy. Some exploratory corrosion tests were made on a few selected pure metals in the hope of finding materials to contain molten uranium-aluminum alloy (2 atom % uranium). The test temperature was 1000°C (1832°F) and the time at this temperature was 4 hr.

Samples were corrosion-tested by immersion in a uranium-aluminum bath contained in a BeO crucible under a blanket of inert gas. Metals tested included beryllium, titanium, iron, zirconium, niobium, and molybdenum. Results indicate that the above metals are not resistant to the uranium-bearing aluminum at 1000°C.

Macro photographs of the test specimens after test are shown in Fig. 14.

DYNAMIC CORROSION TESTING

Forced Convection Loops. The ANP Engineering Group has designed a forced convection loop of 316 stainless steel for operation with sodium. The major components of the loop are near completion. Ultimately it is hoped that this loop will operate with a temperature drop of 1800 to 1250°F and with a velocity

NOT CLASSIFIED
PHOTO NO. Y-2625

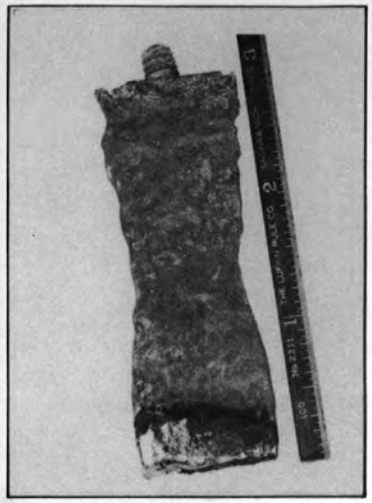

BERYLLIUM

TITANIUM

ZIRCONIUM

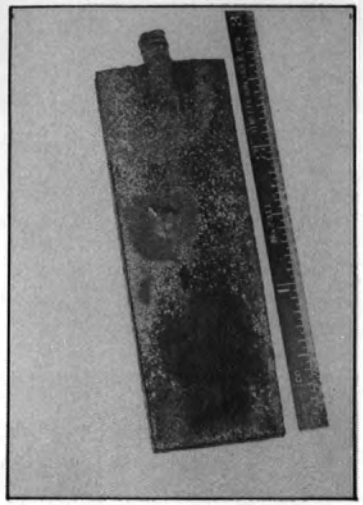

NIOBIUM (COLUMBIUM)

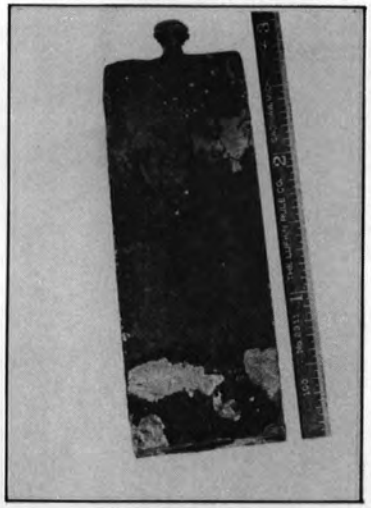

MOLYBDENUM

TANTALUM

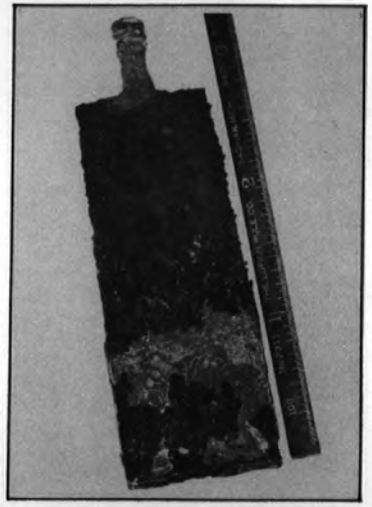

WOLFRAM (TUNGSTEN)

CORROSION SPECIMENS IN MOLTEN U-AL ALLOY FOUR HOURS AT 1000°C

FIG. 14

E. R. BOYD - E. P. GRIGGS

in the test section of 50 ft/sec. The loop has a built-in heat exchanger to reduce external heating and cooling requirements. Conventional type nichrome or kanthal type heating elements will be used to heat the loop, and forced air circulation will be used for cooling. The loop will be equipped with a dump tank into which it can be emptied in case of emergency. The Design Group has ordered eight electromagnetic pumps from General Electric, but initially they plan to begin operations with an electromagnetic pump designed and constructed at Y-12.

Thermal Convection Loops. The thermal convection loops are being operated by the ANP Engineering Group, with metallurgical control and examination to be done by the ANP Materials Group in the X-10 Metallurgy Division.

Experimental Procedure. The thermal convection loops are first cleaned by degreasing and pickling where necessary. They are then filled with filtered sodium and operated under a helium atmosphere at temperatures up to 1500°F for 1000 hr or until failure occurs. Nichrome heating elements are used for heating the loops, and rock wool blanket insulation is used for insulation. At present, temperature differentials between 60 and 100°C are being obtained around the loops.

Chemical Analysis and Metallographic Examination. Immediately after the loops are filled a sample of sodium is taken from the loop for oxygen analysis. After the loop has been operated, a sample of sodium is taken from the top cup for oxygen analysis, and samples are taken from the top and bottom cups for carbon determinations and spectroscopic analyses for corrosion products.

Metallographic specimens will be taken from the pipe and welds in both the hot and cold zones of the loop. These samples will be examined for corrosion and for any evidence of a local build-up of corrosion products.

Auxiliary Equipment. Two thermal-loop filling devices have been constructed, and one is in operation with sodium. In these devices the liquid metal is forced by inert gas pressure through a 5- or 10-μ porous metal filter into the loop. Three pressure vessels to be used as dry boxes have been received and equipped with auxiliary equipment. These dry boxes will be used for loops constructed of materials that cannot be exposed to the atmosphere at test temperatures, and for special tests where any unusual safety hazard exists.

Work in Progress. At present 19 loops have been or are being operated with sodium at Y-12. So far no loops have been examined metallographically. The attached schedule shows the harps now being operated at Y-12 or examined metallographically at X-10.

NO. OF HARPS	MATERIAL	MAXIMUM OPERATING TEMPERATURE (°F)
2	316 stainless steel	1500
2	316 stainless steel	1350
2	304 stainless steel	1350
1	304 stainless steel	1500
1	L-605 cobalt base wrought alloy	1500
4	Nickel	1500
2	347 stainless steel	1350
1	347 stainless steel	1500
2	Low-carbon iron	1200
2	321 stainless steel	1350

Procurement of Material and Loops. The following thermal convection loops are being ordered from the Philadelphia Pipe Bending Company:

QUANTITY	MATERIAL	STATUS
3	310 stainless steel	One complete
3	446 stainless steel	Incomplete
3	Inconel	One complete
3	316 stainless steel ELC	Incomplete
2	V-36 cobalt base wrought alloy	Incomplete
2	L-60 cobalt base wrought alloy	Incomplete
4	310 stainless steel shrouded with 1010 iron	Incomplete
1	V-36 shrouded with 1010 iron	Incomplete
1	L-605 shrouded with 1010 iron	Incomplete

Sufficient pipe-sheet and tube material is being procured to fabricate six to nine harps of each of the following materials:

310 stainless steel	316 stainless steel ELC
405 stainless steel	410 stainless steel
430 stainless steel	430 stainless steel ELC
446 stainless steel	321 stainless steel
Nickel Grade A	Nickel Grade L
Inconel	Inconel X

COMPATIBILITY TESTS OF POTENTIAL FUEL-ELEMENT MATERIALS

Description of Tests. As one step in the selection of materials suitable for use in fabricating fuel elements, compatibility tests have been initiated. These tests will aid in selecting permissible combinations for contact at temperatures of the order of 1100°C.

Appropriate combinations of materials and physical shapes were selected to give the contact surfaces of interest. These materials were then placed in stainless-steel capsules, the capsules were evacuated, and the ends were sealed by welding. The capsules and contents were then hot-swaged at about 1000°C to obtain a 40% reduction in cross section. It was hoped that this step would create intimate contact at newly created surfaces, thus offering maximum opportunity for interaction if a tendency to this was present.

The capsules were heated for 100 hr at 1100°C in a protective helium atmosphere, sectioned, and mounted for metallographic examination (Table 7).

The first capsule to be processed opened at a seam during the final reductions of the swaging operation. The stainless-steel tube showed signs of tearing in the region of the plugged ends in four of seven subsequent runs, causing rejections of several of the tests. The capsule which ruptured at the seam was sectioned without further heat-treatment to observe the effects of the swaging operation. Notes on examination of both as-swaged and heat-treated samples follow. Capsules containing the contact surfaces UO_2-316, BeO-316, UO_2-Cb, BeO-Cb, Be-316, Be-Cb, Be-UO_2, Be-BeO, and Be-Mo are being processed.

TABLE 7

Results of Contact of Potential Fuel-element Materials at 1100°C for 100 hr

METAL COMBINATION	REACTION
Mo - 316	Trace
Mo - 309	Trace
Mo - UO_2	None
Mo - BeO	None
316 - Cb	Medium

Molybdenum—316 Stainless Steel. *As-swaged.* In the structure of the worked molybdenum a flow pattern was evident. The molybdenum was cracked through at several points. Reduction in cross section of the components was not uniform, and there was no evidence of reaction between molybdenum and stainless steel even at points where apparently good contact was made.

Heat-treated. The molybdenum presented a recrystallized structure. Small tears were present at the inner periphery of the stainless-steel layer. There was evidence of formation of a third phase at the Mo-316 interface, extending into both metals. Layer depths were of the order of 1/1000 in.

Molybdenum—309 Stainless Steel. This combination resulted in the same general structures as in the case of Mo-316 in both the as-swaged and heat-treated pieces. Here again a reaction occurred between the molybdenum and the stainless steel during the heat-treatment period.

Molybdenum-UO_2. *As-swaged.* There was reduction of the cross section of the molybdenum, but the surface of the molybdenum was badly cracked. The UO_2 sintered partially, but there were no indications of the formation of a new phase at the interface.

Heat-treated. A molybdenum tube enclosed in a stainless-steel capsule showed a definitely recrystallized structure at its outer periphery. (Indications of reaction with the stainless steel were strong here.) However, the recrystallized structure gradually gave way to an as-worked structure at the inner surface. There were no positive signs of reaction between the molybdenum and the UO_2, but owing to irregularity of the molybdenum surface it was not possible to get an absolute result from this run.

Molybdenum-BeO. *As-swaged.* A worked structure resulted with no indications of a reaction.

Heat-treated. A recrystallized structure resulted with no evidence of reaction between molybdenum and BeO. The same difficulties with irregularity of surface were present as in the heat-treated molybdenum-UO_2 sample.

Columbium—316 Stainless Steel. *Heat-treated.* The swaging operation resulted in considerable flow of the columbium rods contained in the 316-stainless-steel jacket. There was definite evidence of interaction between the columbium and the steel.

POWDER METALLURGY LABORATORY

Laboratory space has been made available and the equipment is beginning to arrive for the powder metallurgy laboratory. The major pieces of equipment to be installed and their expected delivery dates are:

EQUIPMENT	COMPANY	EXPECTED DELIVERY DATE
75-ton hydraulic press	K. R. Wilson	On hand
50-ton hydraulic powder press		To be ordered
20-ton table press	Loomis	November 15
Molybdenum wound furnace		To be ordered
Burrel Globar tube furnace		On hand
High-temperature muffle furnace		To be ordered
40-kw spark-gap converter	Ajax	December 15
6-kw spark-gap converter	Ajax	December 15
Roller air classifier		October 20
Roll rack (for ball mills)		On hand
Cenco screen shaker with screens		On hand
Atmosphere box		To be ordered
MC-275 package vacuum system		November 1
Pulverizer		December 1
Conical mixer		December 1
Analytical balance		On hand

FORMATION OF A POROUS STRUCTURE BY SELECTIVE LEACHING

One of the possibilities for carrying the fuel component of a fuel element is by impregnation of a porous metal layer created on the surface of a metallic tube. This arrangement should furnish the important characteristic of intimate contact between source of heat in the element and a good conductor for removing this heat.

Selective leaching of precipitated carbides from a carburized surface layer of stainless-steel tubing was tried as a means of fabricating the desired porous layer. Preliminary attempts to remove these carbides with Strauss

reagent proved somewhat disappointing. However, further experiments are planned on both the heat treatment of the stainless steel to obtain a more desirable carbide distribution and on media for removal of the carbides.

WELDING LABORATORY

Orders have been placed for an a-c inert-arc welder, a d-c motor generator set for use as an inert-arc welder, and an atomic-hydrogen welder. Delivery is expected on these welders within the next two months.

Negotiations for the purchase of a vacuum dry box are in progress.

Construction of two purification trains for helium and argon is contemplated.

A 35-kw Lepel high-frequency induction unit has been obtained for use in inert-atmosphere and vacuum-brazing research.

Construction of a 600-volt 300-μf condenser-discharge welder for butt-welding of wires and thin-walled tubing is in progress.

Welding of Molybdenum. Preliminary experiments on welding of molybdenum, in which the facilities of the Research Shops were used, have been unsuccessful. Fansteel molybdenum sheet and rod have been welded with a-c and d-c inert arcs using argon and helium of commercial purity. The use of d-c straight polarity with argon or helium was found to be superior to use of a-c. All welds were brittle, a condition which is frequently suggested as being due to a precipitated oxide or other phase at the grain boundaries of the recrystallized molybdenum.

Atomic-hydrogen welds of Fansteel molybdenum sheet were also brittle. Examination of the sheet used in these experiments showed that the material was laminated. These laminates separated upon repeated bending.

Experiments using Climax arc cast molybdenum are to be made.

Welding of Columbium. Preliminary experiments with 0.020-in. Fansteel sheet columbium indicated that this material can be welded. Joints made with a d-c inert arc using helium and argon and an a-c inert arc using argon were relatively strong and showed some ductility as indicated by repeated bend tests.

CREEP-RUPTURE LABORATORY

General. Eight Baldwin lever-arm machines and two screw type stress-rupture machines have been received and erected. Twelve Leeds and Northrup Speedomax-D.A.T. recorder controllers, one Speedomax 12-point recorder, and one 56-point precision indicator unit have been received and installed. At present the operating and control circuits are on temporary wiring pending the delivery and installation of the permanent duct work. Interim operation is directed toward studying the operation and control characteristics of the installations. It is definitely indicated that these systems will maintain the temperature within ±1°C for at least 400 hr, the longest operation to date.

ANP Creep-rupture Testing. High-temperature strength data are very scarce for alloys in sheet or tube form and nonexistent for the temperatures and liquid-metal environments expected in the aircraft reactor. The tests will be made on sheet specimens in inert-gas and liquid-metal environments and at temperatures from 600 to about 1000°C. Since suitable equipment is not available commercially, it is necessary to develop and build this equipment in the area.

Special lever-arm type machines are now under construction. Vacuum and inert-gas chambers are in the final design stage, and the chambers for testing in liquid metal are in the preliminary design stage. If schedules can be met, several tests in each environment should be started during January, 1951.

Since a great deal of pipe and tubing will be used in the aircraft, attempts are being made to develop a creep-rupture test for such shapes. The design must provide for safely holding the liquid metal under pressure either inside or outside the test specimen at elevated temperatures for long periods of time. Also, it would be desirable to provide means to gauge the dimensional change of both the diameter and the length of the specimen during the test.

Creep of Uranium. As part of the general research on metallic uranium and as an aid to reactor design it has been deemed necessary to study the mechanical properties of uranium at elevated temperatures. The Baldwin lever-arm machines and part of the instrument assemblies mentioned previously are for this purpose.

Two uranium specimens have been under stress in hot oil baths for about 700 hr. One sample is stressed to 26,000 psi at 100°C and the other to 21,000 psi at 150°C. The elongation to date is about 2%. Vacuum chambers, pumps, and special furnaces are being procured for the study of the creep of uranium at temperatures up to about 800°C.

A Gaertner cathetometer with a sensitivity of 0.00001 in. and 12 platinum-strip extension gauges have been procured. Plans are being considered for obtaining several strip extension gauges of molybdenum for special purposes. A 20-kw gasoline-driven stand-by electrical-power unit has been procured. A system for the purification of the inert gases is being developed in the ANP Group of the Metallurgy Division.

Uranium will be tested in a vacuum and at temperatures as high as 800°C. In event of failure of the vacuum system with the present ventilating installation the entire building would be contaminated; hence the portion of the ventilating system serving the creep laboratory will be modified.

VI. MECHANICAL PROPERTIES OF PURE METALS

The second part of "A Study of Stress-Strain-Time Functions of Metals" is now in the reproduction stage and will be issued as a memorandum. It contains the results of experimental work on copper at room temperature. Stress-strain-time curves were obtained by various means, suitable to the varying strain rates used. At low straining rates microformer extensometers were used before necking set in. Thereafter an Olsen micrometer gauge, provided with knife edges, was used for measuring the diameters of the test specimens. Time readings were recorded throughout the tests.

At higher straining rates microformer extensometers were used for strains up to 0.25, but at strains higher than 0.25 and at the fastest strain rates a photographic method for recording and measuring load, strain, and time was used. A 35-mm motion-picture camera was set up to photograph the test specimen, a time piece, and a load gauge simultaneously. This is shown in Fig. 15. This auxiliary load gauge, driven by selsyn motors, accurately reproduced the readings of the main load indicator.

The load-strain-time data obtained were worked up into true stress—natural strain—time diagrams. The straining rates could be considered as approximately constant up to natural strains of 0.5 to 0.6. Sections perpendicular to the time coordinate of the three-dimensional diagram then yield the rate of change in true stress with natural strain alone ($\partial\sigma/\partial\delta$). Other sections perpendicular to the strain coordinate correspondingly yield the rate of change of stress with time alone ($\partial\sigma/\partial t$). The true stress—natural strain—time diagrams after long intervals yield surfaces whose tangents $\partial\sigma/\partial t$ approach zero as a limit. The stress-strain curve after very long intervals yields a curve, $\sigma(\delta)$, whose tangents are annotated $(\partial\sigma/\partial\delta)_c$. Corresponding stress values are called $(\sigma)_c$. The $(\sigma)_c$ vs. δ curve is practically identical with the true stress—natural strain curve obtained at exceedingly slow straining rates. In Fig. 16 is a log-log plot of such curves. It may be noted that the curve contains four flexures. It is thought that study of the curve up to a strain of 0.01 with the first two flexures may show correlations with minute structural changes. If this is so, the relationship may throw light on the formation and propagation of dislocations. That these flexures are not accidental has been ascertained by repeated tests using

Not Classified
Photo No. Y-3027

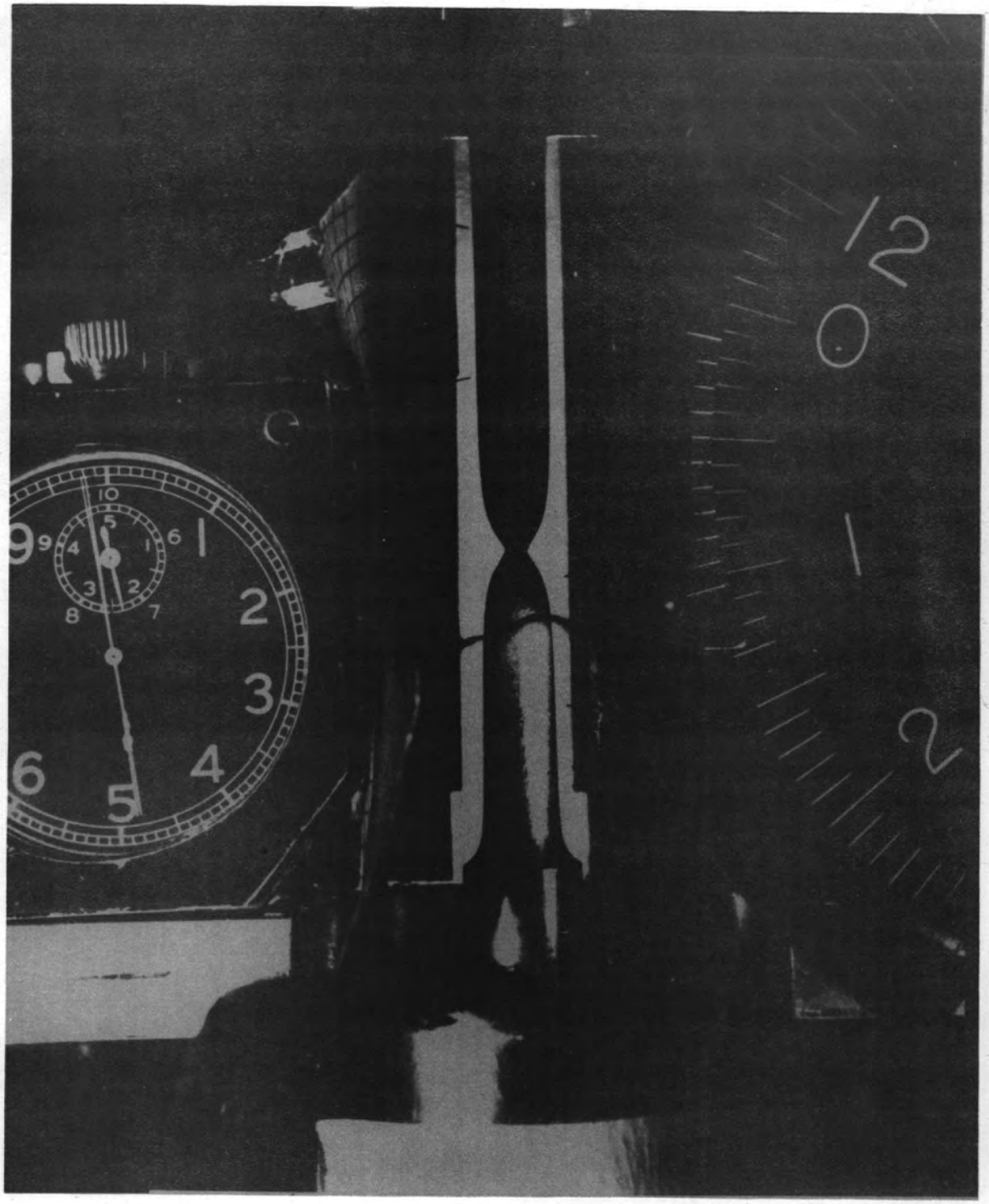

Silhouette of a Copper Specimen During Stress

Fig. 15

NOT CLASSIFIED
DWG. 9377

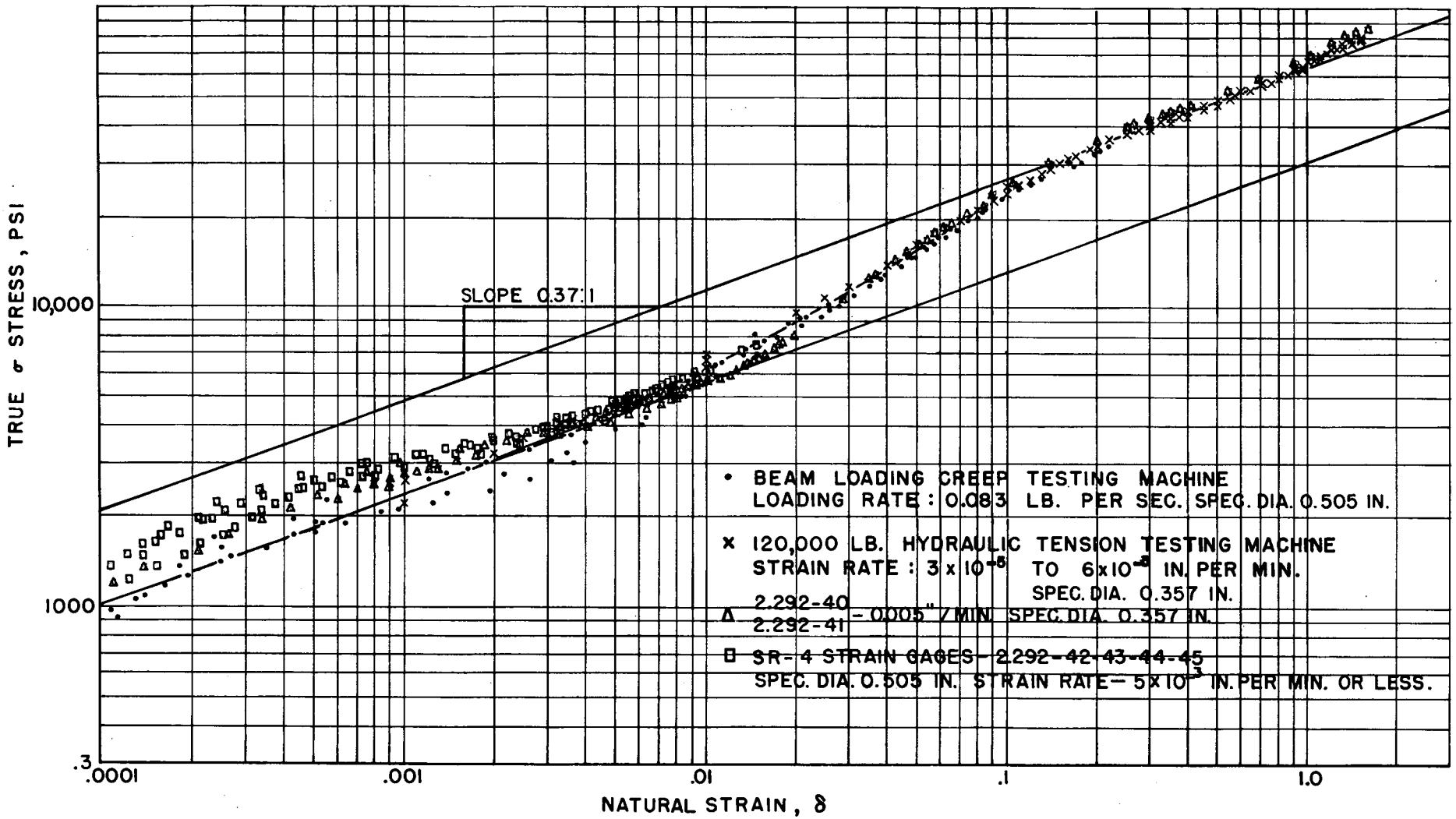

FIGURE 16 TRUE STRESS VS. NATURAL STRAIN DIAGRAM.
OFHC COPPER, ROOM TEMPERATURE.

different types of testing machines, two different types of extensometers, and SR-4 strain gauges. This is demonstrated by three illustrations. The data of Fig. 17 were obtained on the 120,000-lb. hydraulic tensile testing machine and microformer extensometer. Those of Fig. 18 were obtained by a beam-loading type creep-testing machine arranged for tensile testing, and Fig. 19 was obtained from the hydraulic machine, using SR-4 strain gauges. The portion of the curve between strains of 0.01 and 0.15 is of unusual interest. Figure 16 shows that two parallel straight lines conform approximately to the portions of the curve which lie outside these limits. Plotting the values of σ described by the upper straight line less the actual σ values given by the experimental curve, against strain δ, we obtain the curve shown in Fig. 20. This typically skewed probability curve indicates very strongly an increase in stress inversely proportional to some process of depletion and is thought to indicate a second group of progressive structural changes in the strained metal. The process appears to start with 100% unprocessed metal (with reference to the supposed second group of changes) at a strain of about 0.005 and a rapidly increasing stress differential. This reaches a maximum at a strain of 0.03 and then slowly decreases as depletion of unprocessed metal progresses. There is reason to believe that above a strain of 0.15 the process is not completed but continues at an increasingly slow rate to a saturation point at about 0.37 where no more unprocessed material is available. A third stage of deformation, characterized by necking, begins at this point and probably continues linearly (on the log-log plot) until fracture occurs. The last flexure at a strain of about 1.0 is in all probability due to the rapid increase in strain rates which reaches tremendous magnitudes above a strain of about 1.0. This last increase in stress above the linear relationship is a gratifying, though not by itself adequate, confirmation of the hypothesis which prompted the present experiments to be undertaken. It is suggested that the slopes of the $(\sigma)_c$ curve and particularly the locations of its first three flexures may change with neutron exposure and may thus throw light on radiation damage problems.

An approximate expression for the $(\sigma)_c$ curve is

$$\sigma_c = [K_1 + (K_3 - K_1)\epsilon^{-0.03/\delta}]\delta^m \qquad (1)$$

For values of strain below 0.01 this expression reduces to $K_1\delta^m$ and above 0.15 to $K_3\delta^m$, which are identical in form with the commonly used expression for

NOT CLASSIFIED
DWG. 10264

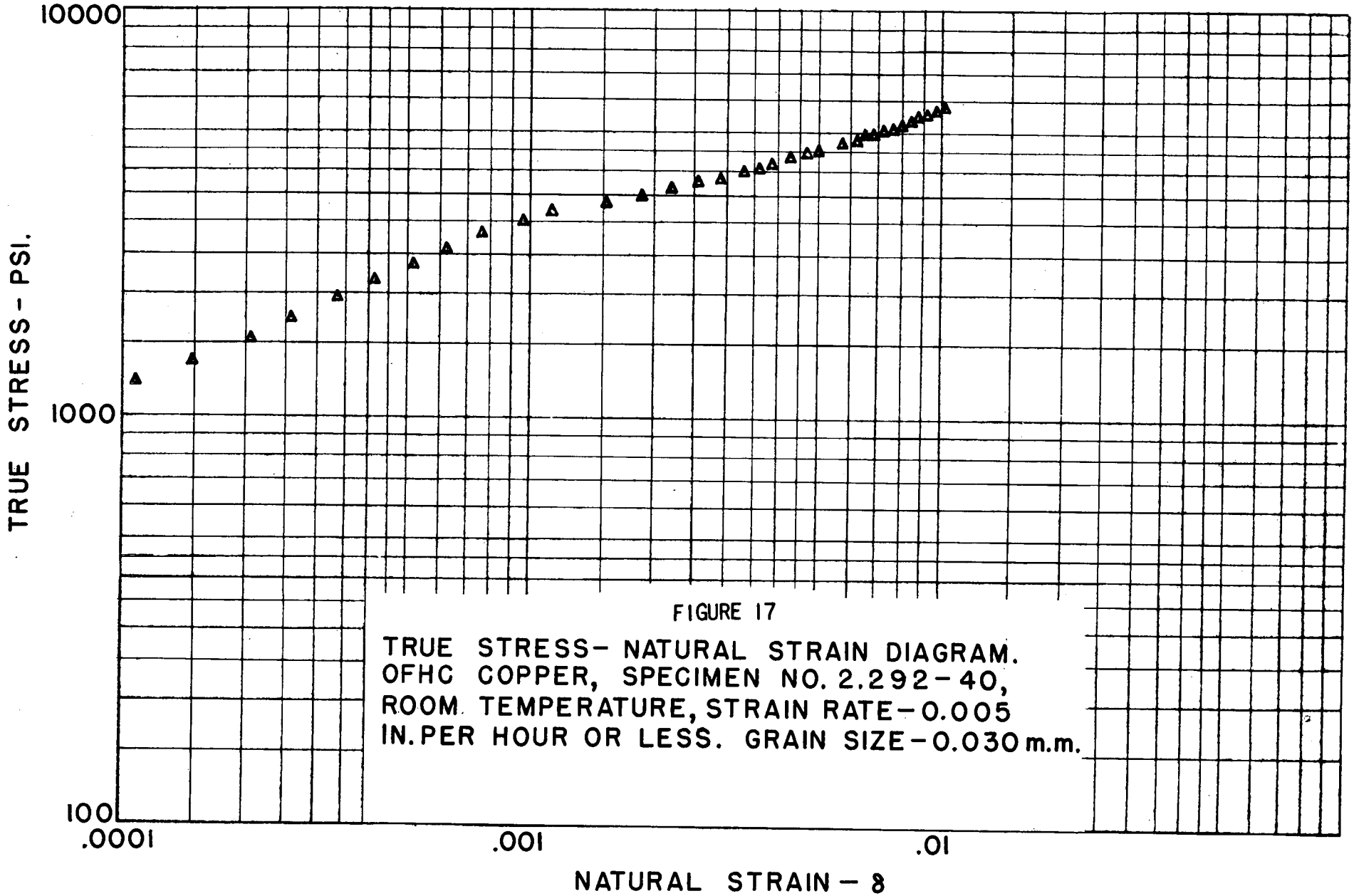

FIGURE 17

TRUE STRESS- NATURAL STRAIN DIAGRAM. OFHC COPPER, SPECIMEN NO. 2.292-40, ROOM TEMPERATURE, STRAIN RATE-0.005 IN. PER HOUR OR LESS. GRAIN SIZE-0.030 m.m.

NOT CLASSIFIED
DWG. 9374

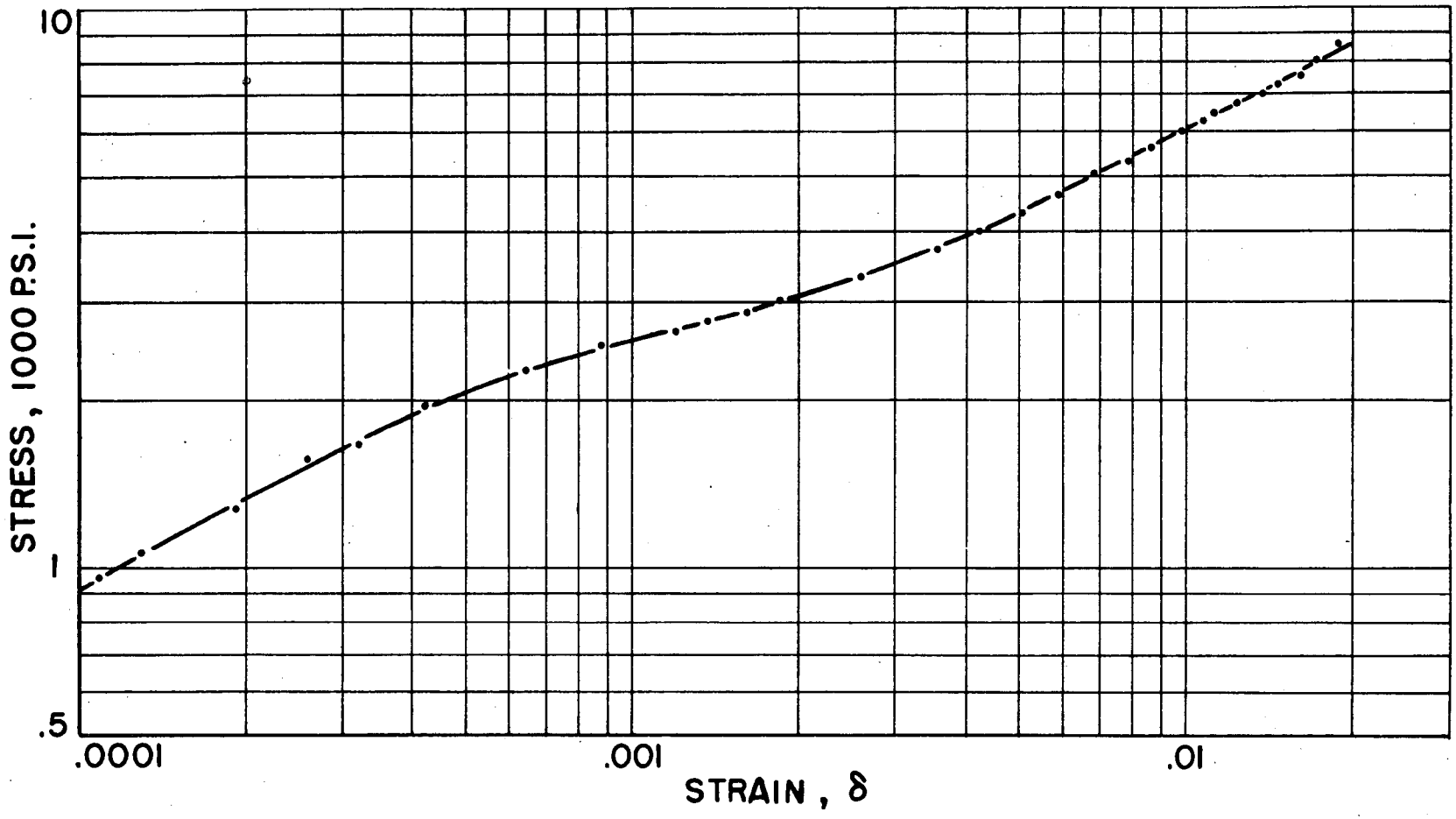

FIGURE 18 - TRUE STRESS - NATURAL STRAIN DIAGRAM, OFHC COPPER, SPECIMEN NO. 2.2911, ROOM TEMPERATURE, BEAM LOADING TYPE CREEP TESTING MACHINE. LOADING RATE: ¼ LB. PER MIN. (1500 PSI. PER HOUR)

NOT CLASSIFIED
DWG. 10265

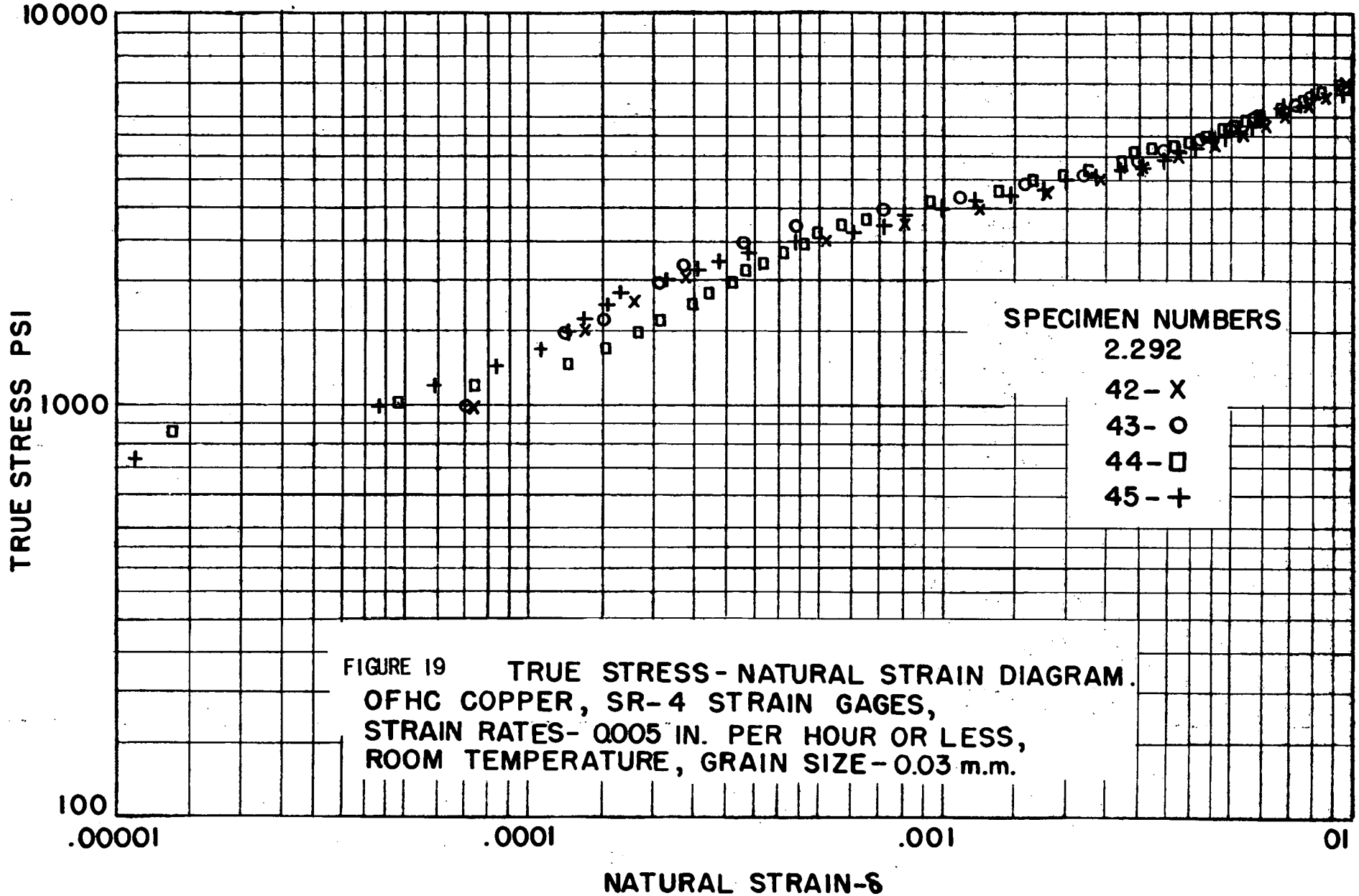

FIGURE 19 TRUE STRESS - NATURAL STRAIN DIAGRAM.
OFHC COPPER, SR-4 STRAIN GAGES,
STRAIN RATES- 0.005 IN. PER HOUR OR LESS,
ROOM TEMPERATURE, GRAIN SIZE - 0.03 m.m.

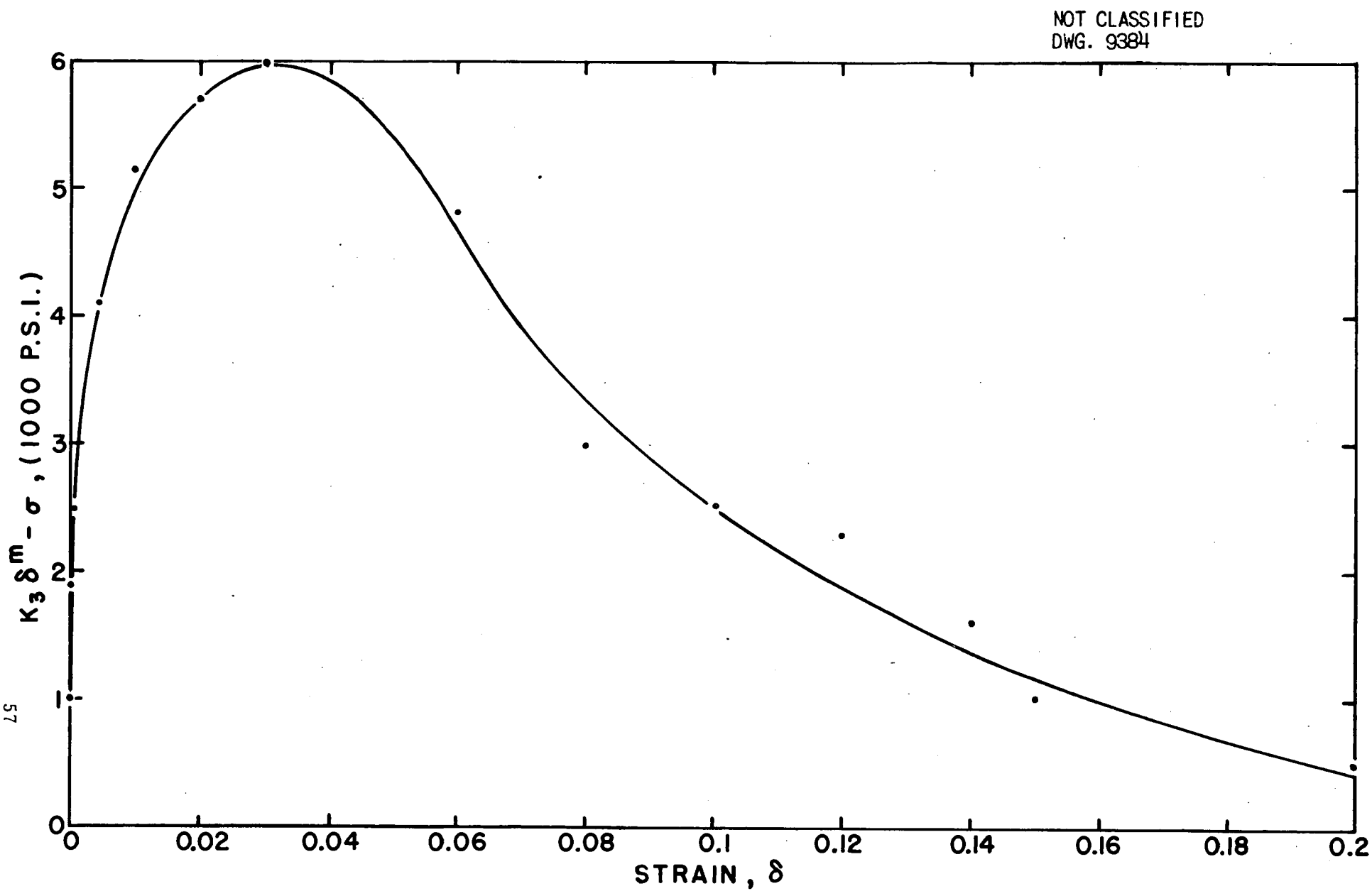

FIGURE 20 - DEVIATIONS OF $K_3\delta^m$ FROM MEASURED STRESS, σ. OFHC COPPER, ROOM TEMPERATURE.

strain-stress curves. It may be noted that whenever possible the curve itself and not an approximate expression for it should be used.

Sections giving curves of stress vs. time for a number of values of strain are shown in Fig. 21. From these the time functions of the stress are obtained,

$$\sigma - \sigma_c = B\delta^u t^{-b} \tag{2}$$

Numerically, the variation in stress with strain and time is given by

$$\sigma = \sigma_c + 8.8\delta^{0.7} t^{-0.38} \tag{2.1}$$

for copper at room temperature. σ_c is given by the curve in Fig. 16 or approximately by the expression

$$\sigma_c = [K_1 + (K_3 - K_1)\epsilon^{-0.03/\delta}]\delta^m = [31 + 33\epsilon^{-0.03/\delta}]\delta^{0.37} \tag{1.1}$$

By partial differentiation of Eq. (2) the expressions f_δ and f_t are obtained. The change in stress with strain and time simultaneously then is

$$d\sigma = (vf_\delta + f_t)\ dt$$

Level curves of the stress-strain-time functions obtained at essentially uniform strain rates are given by

$$v = -\frac{f_t}{f_\delta} = \frac{\frac{b}{t}(\sigma - \sigma_c)}{\frac{u}{\delta}(\sigma - \sigma_c) + \frac{m}{\delta}\sigma_c + \Gamma} \tag{3}$$

where

$$\Gamma = 0.03(K_3 - K_1)\delta^{(m-2)} \times \epsilon^{-0.03/\delta}.$$

These are called $(\sigma)_v$ level curves in order to denote the restriction of uniform strain rate. The numerical value of $(m/\delta)\sigma_c + \Gamma$ can be obtained from the curve in Fig. 16. We therefore can write

$$v = \frac{\delta}{t}\frac{b}{u + \frac{\Lambda}{(\sigma - \sigma_c)}} \tag{3.1}$$

NOT CLASSIFIED
DWG. 9378

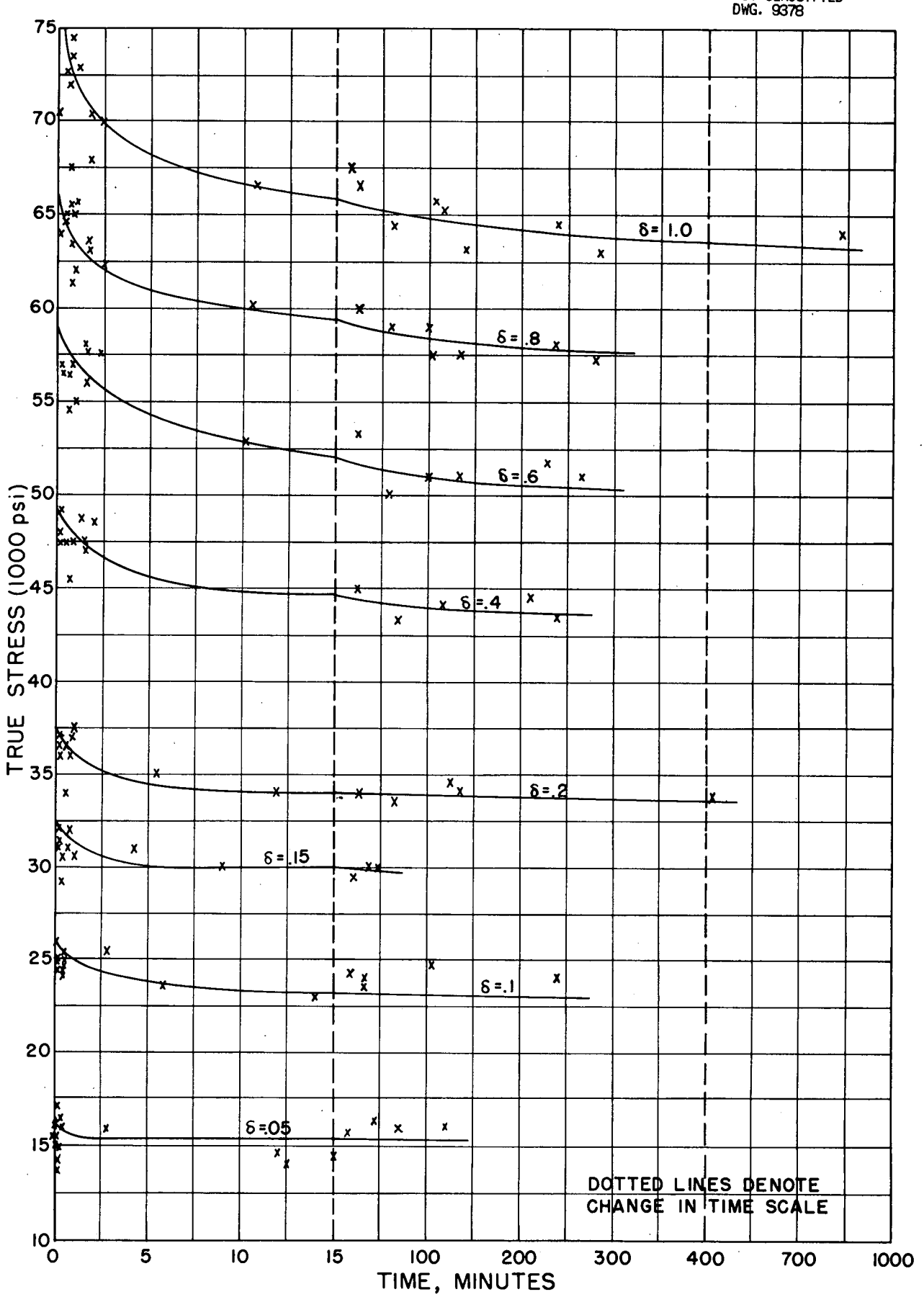

FIGURE 21 – OFHC COPPER, 292 SERIES
STRESS-TIME SECTIONS AT
CONSTANT STRAIN

where λ is obtained from the slope of the curve in Fig. 16. By hypothesis, these curves are related to the creep curves with deviations which depend upon successive time derivatives of the strain rates. The creep rates are derived from the general expression for change in stress with strain and time when no restriction is placed on the straining rate. This more general expression is

$$d\sigma/dt = vf_\delta + f_t + af_v + \dot{a}f_a + \ldots \tag{4}$$

which gives the creep curves at constant stress when σ is kept constant. By setting $d\sigma = 0$, we obtain

$$v = -\frac{f_t}{f_\delta} + \frac{af_v + \dot{a}f_a + \ldots}{f_\delta} = -\frac{f_t}{f_\delta}(1 + \zeta) \tag{5}$$

where

$$\zeta = (af_v + \dot{a}f_a + \ldots)/f_t$$

The relation between the $(\sigma)_v$ level curves and the creep curves, denoted $(v)^c$ in order to indicate a constant stress condition, is apparent from Eq. (5). The ζ function has so far not been determined, but the correspondence between the two sets of strain rates is indicated in Table 8 and Fig. 22. Table 8 gives corresponding values of natural strain rate and time for a particular experimental creep curve at a slowly increasing stress to about 21.7. The strain rates of the $(\sigma)_v$ level curves in this δ, t neighborhood are given by the first term of the creep equation

$$(v)^c = \frac{\delta}{t}\,\frac{0.38}{0.7 + \lambda/(21.7 - \sigma_c)}(1 + \zeta) \tag{6}$$

Values of λ and σ_c for a series of strains are obtained from Fig. 16. The rates v for the annotated time values are calculated and entered alongside the creep rates. It is seen that initially, that is, on the transient, the creep rates are several orders of magnitude less than the strain rates given by the level curves, which is expected from the hypothesis. During the period of secondary creep the rates are of the same order of magnitude, but the creep rates are decreasing more slowly than the rates of the $(\sigma)_v$ level curves.

NOT CLASSIFIED
DWG. 10266

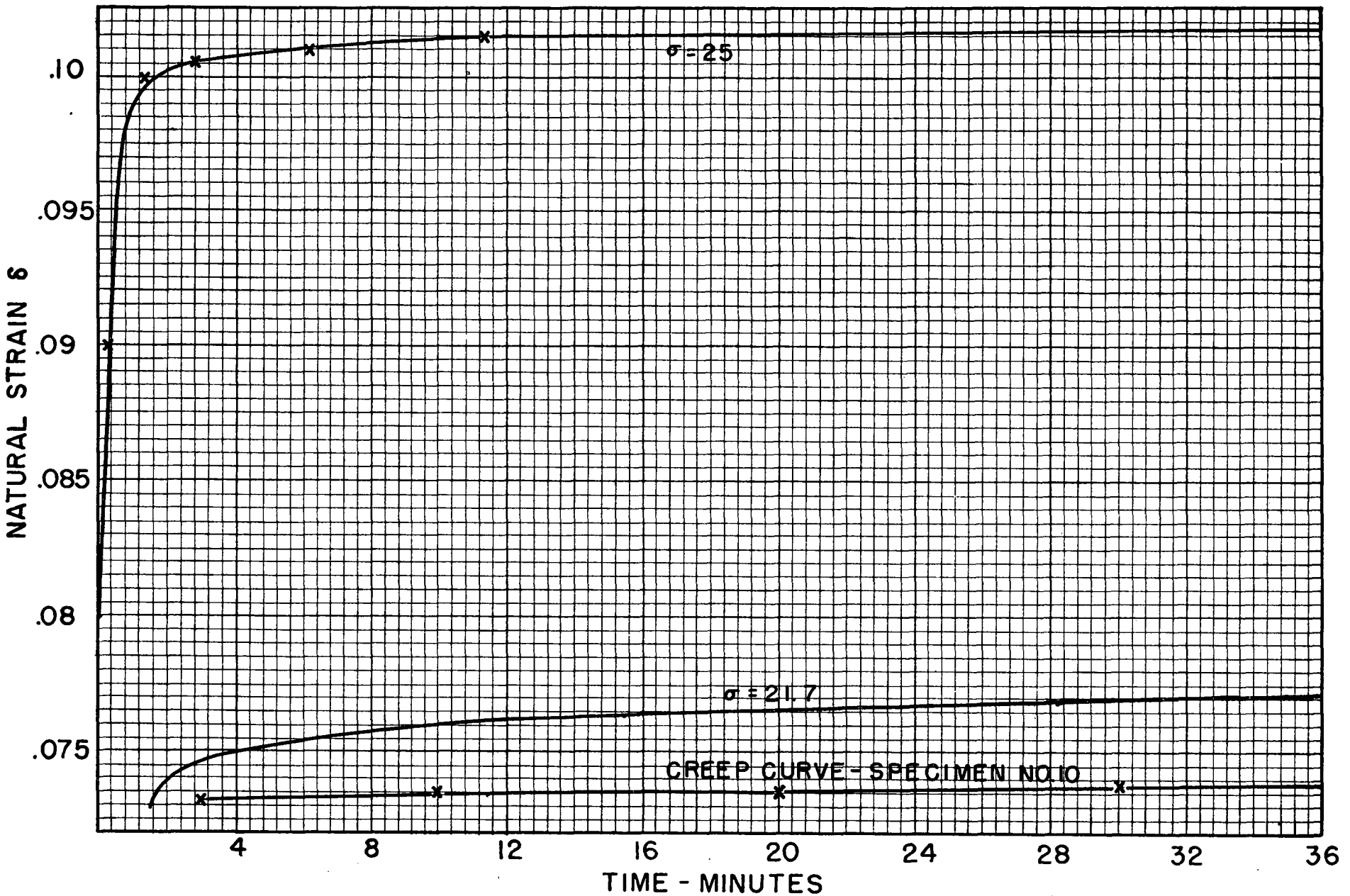

FIGURE 22 LEVEL CURVES OF THE $(\sigma)_V$ SURFACES, OFHC COPPER, ROOM TEMPERATURE

This is entirely to be expected, for since the rates are always slowing up, the effect of the acceleration term ζ must tend to vanish after very long periods. The rates of the level curves will reach zero ahead of the creep rates. The creep curve thus tends to approach the level curve as a limit after long periods. A rational method of extrapolating creep curves is thus at hand. The creep curve lies within the level curve up to the region of necking or internal grain separation.

A fact that must also be considered is that the creep curves were obtained at constant load. This has the effect of increasing the value of the first term of Eq. (6) above that of the level curve and hence of increasing the creep rate. Constant-stress creep rates would be smaller than the constant-load creep rates given in the third column of Table 8.

Further studies have been planned, but experimental work will be resumed only after a decision has been reached concerning the pertinency of further work to the general ORNL research objects.

TABLE 8

Comparison of Creep Curves and of Level Curves of the $(\sigma)_v$ Surface

CREEP TEST NO.	LOAD (psi)	TIME (min)	STRAIN (δ)	SLOPE OF CREEP CURVE, EXPERIMENTAL $\left(\frac{\Delta\delta}{\Delta t} \times 10^8\right)$	SLOPE OF LEVEL CURVE, CALCULATED FROM TENSILE-TEST DATA $\left(\frac{f_t}{f_\delta} \times 10^8\right)$
					$\sigma = 21.0$
10	20,609	3	0.0730	2,400	120,000
		6		2,000	42,000
		10		1,600	21,100
		30		900	5,000
		60		500	2,000
		90		400	1,050
		180		257	405
		500	0.07443	68	98
		1,000	0.07463	29	39
		2,000	0.07481	11	15
		3,000	0.07471	9	9
		4,000	0.07497	7.5	6
		6,000	0.07508	4.7	3.4
		12,000	0.07533	3.6	1.3
		30,000	0.07575	1.5	0.4
		50,000	0.076		
					$\sigma = 29.0$
19	29,100	180	0.1454	10,000	900
		1,000	0.1495	3,000	100
		3,000	0.1527	100	20
		6,000	0.1553	65	9
		12,000	0.159	45	3.5
		30,000	0.1639	20	1
		50,000	0.1675	16	0.5

TABLE 8 (Cont'd)

CREEP TEST NO.	LOAD (psi)	TIME (min)	STRAIN (δ)	SLOPE OF CREEP CURVE, EXPERIMENTAL $\left(\frac{\Delta \delta}{\Delta t} \times 10^8\right)$	SLOPE OF LEVEL CURVE, CALCULATED FROM TENSILE-TEST DATA $\left(\frac{f_t}{f_\delta} \times 10^8\right)$
					$\sigma = 25$
16	24,982	100	0.1045	5,500	1,300
		500	0.1068	193	140
		1,000		86	65
		2,000		46	22
		3,000		30	13
		4,000		23	9
		6,000		16	5
		12,000		8	2
		30,000		3	0.6
					$\sigma = 35.0$
15	35,000	1,800	0.292	5,600	880
		2,300	0.304	4,000	670

VII. SERVICE WORK

Aluminum-Silicon Coated Slugs. The Chemical Technology Division of Oak Ridge National Laboratory asked the Metallurgy Division to prepare 100 uranium-aluminum slugs 1.4 in. in diameter and 8 in. long for use in development of a process for dissolving P-10 slugs. These slugs were prepared by casting a 4-in.-diameter ingot of 7½% uranium content and extruding into 1.4-in.-diameter rod. The rod was machined into slugs of the proper length, 50 of which were returned to be dipped in Al-Si eutectic for coating with approximately 16 g of Al-Si. It was found that the slugs could be coated satisfactorily if they were thoroughly cleaned by etching in NaOH solution and preheated to approximately 600°C before being dipped in the molten Al-Si bath.

Since the P-10 slugs thus far loaded into the Hanford Reactor have been cast slugs, an additional 72 slugs were prepared and coated with Al-Si for comparison with the extruded material. The Chemical Technology Division found that the extruded slugs dissolved in 4 *N* HNO_3 at a much faster rate than the cast slugs. In order to determine the effect of working upon the dissolution rate, it was requested that cast slugs be worked slightly by cold-rolling. Accordingly, two slugs of cast 7½% U-Al were cold-rolled from 1.25 to 1 in. diameter (36% reduction in area). In order to have comparable samples, two extruded slugs were treated in the same way as the cast slugs. One slug of each type was fully annealed while the other was left in the strained state. It was found that the extruded rods again dissolved at a faster rate than the cast slugs, but the worked cast slug dissolved faster than the one in the cast condition.

As might be expected, examination of the microstructure revealed a possible explanation for the different rates of dissolution. In the cast slugs, both before and after working, the eutectic was distributed around the large primary grains of aluminum. In the case of the extruded material, the eutectic was broken up and uniformly distributed in a matrix of aluminum. It is known that the compound UAl_4 is much more readily attacked by acid than is pure aluminum. Thus with a more random distribution of compound particles in the extruded material a faster and more uniform attack by the HNO_3 might be expected.

Preparation of 5% Molybdenum—Uranium Alloy Sheet and Rod. The Metallurgy Division was requested to furnish 15 pieces of 5% Mo—U alloy to be used in connection with experiments being conducted by the University of California Radiation Laboratory. The material furnished was as follows:

6 pieces	3/16 by 4 by 24 in.
6 pieces	1/8 by 4 by 24 in.
3 pieces	1/2 in. dia. by 36 in. long

The flat plates were hot-rolled from 1- by 4- by 6-in. castings, and the rods were extruded to 0.860 in. diameter from a 3-in.-diameter by 6-in. billet, then hot-rolled to size.

In the initial phase of the work it was found that the alloy could be rolled satisfactorily in the gamma phase, but when the gamma-quenched material was given approximately 25% reduction in the cold-finishing passes, one of the 3/16-in. plates cracked during rolling, and three of the remaining 3/16-in. plates failed five days later. A typical failure is shown in Fig. 23. All the 3/16-in. plates, cold-rolled approximately 25%, and three of the 1/8-in. plates, cold-rolled approximately 15%, had split lengthwise within 10 days. Cold-rolling of the extruded rod gave similar results except that the rods cracked radially into pieces as short as 1/2 in. in length.

The final procedure used in the preparation of the required material was as follows:

1. Sheet ingots of uranium containing 5% molybdenum were melted and cast in vacuum in an induction furnace. The ingots were cast into vertical graphite molds.

2. After cropping the shrink head, the plates were heated to 850°C in a salt bath of Houghton's Liquid Heat N.D. and held for 30 min.

3. The plates were then rolled in a 6- by 10-in. two-high mill to within 0.010 in. of the final size with reductions of about 0.050 in. per pass. The metal was reheated after about four passes to maintain the required temperature. The plates were water-quenched after the final pass.

4. The plates were finish-rolled cold in a 20- by 30-in. two-high mill.

[redacted]
Photo No. Y-2236

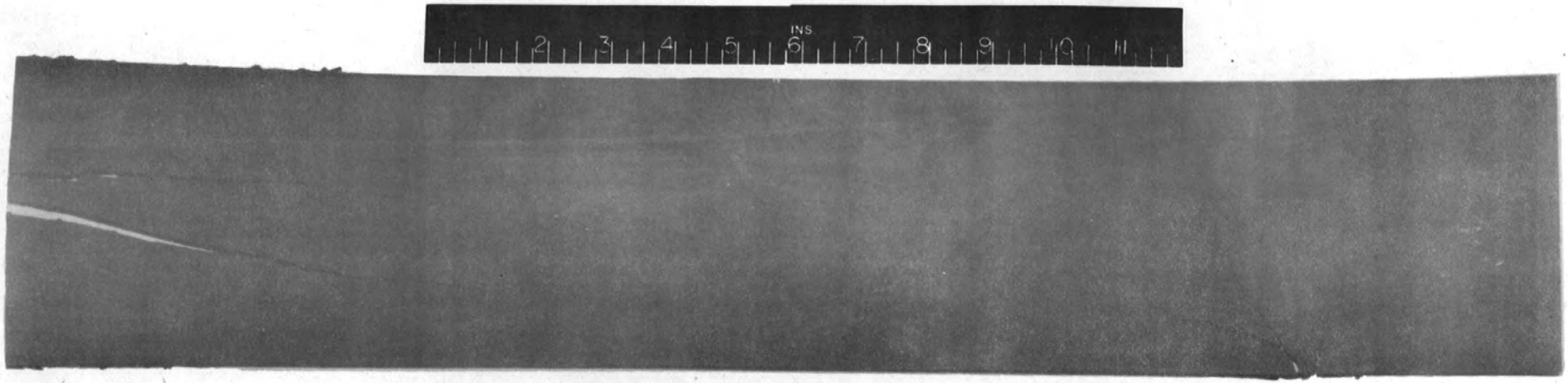

ROLLED PLATE OF U-MO ALLOY
Hot rolled at 850°C to 0.250 in.- Cold rolled to 0.1875 in.

Fig. 23

5. The cold-finished plates were annealed at 850°C for 30 min in an argon atmosphere and water-quenched.

6. The annealed plates required an additional straightening in the 20- by 30-in. mill.

The 1/2-in.-diameter rod was prepared by extruding a cast billet, 3-1/16 in. in diameter by 6 in., to 0.860 in. diameter at 900°C. The resulting rod was reheated to 850°C, rolled to size, and water-quenched. The extrusion was somewhat similar to that of pure uranium except that higher pressures were required. The surface of the extruded rod had essentially the same appearance as uranium previously extruded in the gamma phase and with the same die. The pressure required for extrusion was of the order of 125,000 psi as compared to 64,000 psi required for the same size uranium billet at 850°C.

The failures encountered in the rolling operations appeared to be due to a phase transformation, i.e., the transformation of the retained gamma phase to the stable alpha phase plus an unknown phase induced by the cold-rolling. The annealed material was quite soft (Vickers hardness number 140), but it hardened rapidly upon working, as shown in Fig. 24. There is also evidence of a hardness increase with room-temperature aging immediately after cold-working. The cold-worked material was shown by means of an X-ray diffraction pattern to consist of alpha uranium.

Fabrication of Heater for Pile Fluxmeter. The Physics Division of the Oak Ridge National Laboratory requested the Metallurgy Division to explore the possibility of fabricating an enriched uranium heater of the aluminum—aluminum-uranium alloy sandwich type to be used in a small pile fluxmeter. The required heater core, made from a 1% uranium-aluminum alloy, would be 2 mils thick by 9/16 in. by 1-3/8 in. The core would be enclosed in a 5-mil 2S-aluminum envelope.

It is necessary to develop a method to determine the location and physical outline of the uranium core within the sandwich. The present work has been directed toward developing a fabrication procedure that will produce a rectangular core of the required dimensions. A 7½% uranium-aluminum alloy has been used for this work since the boundary between the frame and the core can easily be distinguished by use of a radiograph of this material.

[redacted]

DWG. 10313

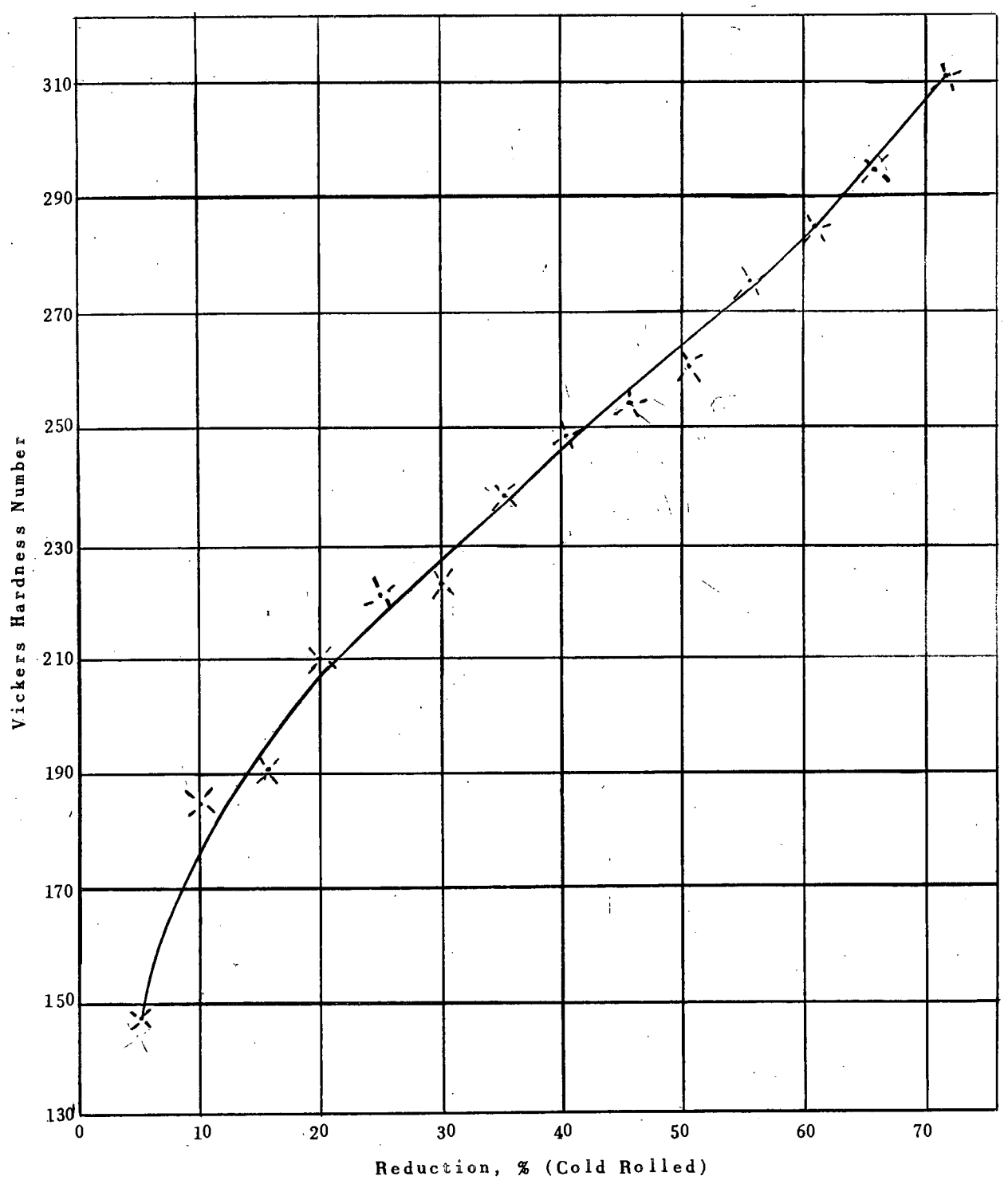

Figure 24

Rate of Work Hardening of 5% Mo-U Alloy

The method of fabrication developed is as follows:

1. A 3/16-in.-square window is punched in a 0.044-in. piece of 2S aluminum, and the window is filled with a 3/16-in.-square by 0.044-in. piece of alloy punched with the same die.

2. The frame with the alloy insert is cross-rolled and then end-rolled to give a 9/16- by 11/32-in. core.

3. The frame containing the core is lined with a scriber and then a pencil.

4. The top and bottom sheets of 2S aluminum are brushed with a wire brush, applied to the center frame by notching, spot-welding, or stapling, and then lined to agree with the lines on the frame.

5. The sandwich is then hot-rolled to the desired thickness.

This lining method has been satisfactory in locating the alloy core in only one of six sandwiches fabricated. The width of the core appears easy to to control in producing parallel sides, but considerable length variation that did not agree with the lines on the cover sheet has been experienced. Further work is in progress in the direction of reducing the amount of rolling necessary after the cover sheets are assembled. This should give better control of the length of the core.

Uranium Melting. Uranium metal is rather difficult to roll, especially when large reductions are needed. It would be desirable when rolling foil or thin sheet to start with a relatively thin ingot. To prove the feasibility of casting thin-sheet ingots of uranium, a number of castings were made in graphite molds 1/8 by 4-1/2 by 8 in. The casting was done in a vacuum furnace, using a graphite-bottom pouring crucible which drained into a stationary vertical mold. A good surface was obtained and the ingot was considered satisfactory.

Thin-wall cylinders of uranium were cast in various sizes. Three cylinders, 6 in. long with a wall thickness of 0.20 in. and having outside dimensions of 2.025, 2.575, and 3.125 in., respectively, were cast in graphite molds. These sizes will permit a concentric arrangement of the tubes.

Welding Laboratory Service Work. Closing the ends of the Chalk River aluminum fuel rod was accomplished by a-c argon-arc welding, and the requirement of a leak-tight joint was met. The leak test was performed by pressure-testing with dry nitrogen.

A preliminary study of vacuum-furnace brazing of copper to copper and copper to uranium was performed for the MTR group, using a 2-in. resistance-heated tube furnace. Copper-to-copper vacuum-furnace brazing was found feasible with test specimens using copper-silver eutectic brazing alloy. When tried with uranium, formation of a brittle intermetallic phase and lack of flow of the brazing alloy were observed. Vacuum brazing of a copper-uranium picture-frame assembly will be attempted in a larger furnace.

Service Work of the MTR Group. The following service work was performed by the MTR Group:

1. Four large pieces of 347 stainless steel were stress-relieved for the Central Shops.

2. Five 1/8-in. silver plates were rolled for Y-12.

3. Three cadmium sheets were rolled to 0.015 in. for Y-12.

4. Two small sheets of platinum were rolled to 0.015 in. for Y-12.

5. Two plates of 1/4-in. Boral were rolled to 1/8 in. for the Reactor Technology Division.

Miscellaneous. Additional service work performed for various divisions at ORNL and groups within the Metallurgy Division includes the following:

1. Preparation of two melts of 5% Si—95% Fe to be used by the Physics Division for growing single crystals.

2. Preparation of an ingot of 50% Fe—Co for the Physics Division.

3. Preparation of U-Zn, Pb-Bi, and U-Al alloys for liquid-metals work.

4. Preparation of alloys of silver with Cd, In, Sn, and Sb for internal friction measurements.

5. Preparation of samples of Armco iron with random orientation and with a grain size of 10 to 20 microns for the Physics Division.

6. Fabrication of a number of copper tubes with an internal layer of bismuth to be used as counter tubes by the Health Physics Division.

7. Fabrication of one Chalk River fuel assembly.

[redacted]

METALLURGY DIVISION PERSONNEL

AS OF NOVEMBER 1, 1950

Abrams, L. A.
Adams, R. E.
Adamson, G. M.
Andersen, A. G. H.
Banker, L. E.
Beaver, R. J.
Billington, D. S.
Blacksher, F. M.
Blewitt, T. H.
Bomar, E. S., Jr.
Borie, B. S., Jr.
Boss, G. H.
Boyd, E. R.
Boyle, E. J.
Brasunas, A. D.
Bridges, W. H.
Buker, D. O.
Carr, H. T.
Childress, K. A.
Coltman, R. R., Jr.
Cooley, G. E.
Crouse, R. S.
Cunningham, J. E.
Cutcher, C. F.
Day, R. B.
Drosten, F. W.
Easton, D. S.
Erwin, J. H.
Feldman, M. J.
Flynn, J. B.
Frye, J. H., Jr.
Fulton, T. W.
Glasgow, L. G.
Goldston, G. D.
Gray, R. J.
Griggs, E. P.
Hamby, D. E.
Hix, J. N.
Howe, J. T.
Hudson, R. J.
Jacox, D. J.
Johnson, R. W.
Jetter, L. K.
Layne, E. E.
Leslie, B. C.
Manly, W. D.
Miller, E. C.
Murray, G. T.
Ogle, J. C.
Oliver, R. B.
Patriarca, P.
Poe, D. B.
Pope, J. E.
Rosson, D. E.
Smith, C. D.
Smith, C. L.
Smith, G. P., Jr.
Taylor, W. E.
Thomas, M. J.
Trotter, L. R.
Turner, J. P.
Wallace, H. J.
Wallace, R. M.
Weaver, C. W.
Webb, R. S.
Williams, R. O.
Wilson, J. C.
Woods, J. W.
Zukas, J. C.

[redacted]